Coupled effects of tide and swell on water renewal in a meso-tidal channel lagoon: Case of the Toliara Lagoon (Madagascar)

Sow Moustapha, Cristèle Chevalier, Bamol Sow, Marc Pagano, Jean-Luc Devenon

Version of Record: https://www.sciencedirect.com/science/article/pii/S0272771421003164
Manuscript_aab860a29537a7edc69cf39fb4fda0e5

Coupled effects of tide and swell on water renewal in a meso-tidal channel lagoon: Case of the Toliara Lagoon (Madagascar)

Sow Moustapha[*], *C. Chevalier*[*], *Bamol Sow*[**], *Marc Pagano*[*], *Jean-Luc Devenon*[*]

[*] Aix Marseille Univ, Université de Toulon, CNRS, IRD, MIO, 13288 Marseille, France

[**] *Université Assane SECK de Ziguinchor, Ziguinchor - Sénégal*

Abstract

In this article, based on the example of the Toliara lagoon in Madagascar, we identified the major impacts of the two main drivers of the water renewal in a typical channel lagoon: the tide and the swell breaking on the reef. For this purpose, we applied the numerical model Croco which is based on ROMS-AGRIF and uses a realistic and high-resolution configuration. The validation was performed with in situ ADCP data, then, realistic and sensitivity simulations were run to infer tides and waves role in ocean-lagoon exchanges and to estimate water age and water origin. The modelling approach adopted enabled an understanding of the effects of swell and tide on the water renewal. During low wave conditions, tide and waves counteract each other on cross-reef flow: the cross-reef inflow tends to increase with waves breaking on the reef, whereas cross-reef flow tends to decrease or to be outflowing with tidal action. Hence, the lagoon-ocean exchange is reduced and is at a minimum when wave height reaches 0.85 m and the tide has minimum amplitude. During high wave conditions, both tide and waves increase ocean-lagoon exchanges by increasing the cross-reef inflow, whereas during low wave conditions, the cross-reef flow is mainly outward with increase with tidal amplitude and decrease with wave height until the threshold of 0.85 m.

Introduction

Located at the coast/ocean interface and separated from the ocean by an alive coral reef barrier, the coral reef-lagoon systems, provide a unique habitat for numerous species as well as a natural and efficient protection against erosion processes and submersion events induced by storms or tsunamis (Fernando et al., 2005). However, the reef colonies and all their benefits for biological and human populations are threatened by the combined effects of increasing anthropic pressure and climate change (sea level rise, acidification, warming, etc, Hoegh-Guldberg et al., 2008), which induce bleaching and coral mortality (Hughes et al. 2003; Pandolfi et al. 2003). The health and the resilience of the lagoon ecosystems depend on the lagoon ability to dampen the deleterious climate change effect through biogeochemical processes and lagoon/ocean exchanges (Carassou, et al., 2010; Szmant, 2002; Andréfouët et al. 2001; Chevalier et al., 2015b). Since their ecological functioning is directly linked to their hydrodynamics (Andréfouët et al., 2006; Lucas et al., 2009), they constitute striking examples of interacting processes: hydrodynamic circulation is driven by the coral reef barriers separating the lagoon from the surrounding ocean, and conversely, the coral reef health depends on this circulation.

Understanding the reef-lagoon hydrodynamics remains a challenge for coastal oceanographers since these systems are potentially exposed to multiple physical forcing such as tide, waves, wind, coastal currents, rainfall, river discharges and evaporation, density-driven currents between lagoon and ocean (Atkinson, et al., 1981). However, in meso and macro-tidal lagoons, the circulation and the ocean-lagoon exchanges are primarily driven by the tidal oscillations which fill the lagoon during the flood and empties it during the ebb, inducing water renewal through passages mainly (Wolanski, et al, 1993; Andréfouët, et al., 2001; Hench et al., 2008; Taebi et al., 2011; Sous et al. 2017). The offshore wave forcing plays indirectly a secondary but significant role (Angwenyi and Rydberg, 2005; Hoeke, et al., 2013): when the oceanic waves arrive on the coral reefs barrier, the forereef slope and the shoaling induce a transfer of their energy toward infra-gravity or superharmonics waves (Masselink, 1998; Pomeroy, et al., 2012, Aucan et al., 2017) and toward cross-reef inflow which velocity may be comparable to the tidal velocity (Hearn and Parker, 1988; Symonds et al., 1995; Hardy and Young, 1996; Kraines et al., 1999; Tartinville an Rancher, 2000; Monismith et al., 2013, 2015). These processes are also modulated by the dissipation by bottom friction along the coral reef (Gourlay, 1996a; Gourlay, 1996b; Massel and Gourlay, 2000) and interaction with co- or counter-currents (Roberts and Suhayda, 1983).

Thus, depth, external slope and roughness of the coral reef barrier are important controlling factors for these processes. The lagoon geomorphology (reef barrier length; number and size of reef-openings …) also plays an important role on the relative importance of these forcings in lagoon water renewal. Hence, in channel lagoons

(where the coral reef length is high compared to passage width) the lagoon water is mainly driven inside due to breaking wave flow (e.g. about 80% in the Ouano lagoon, New Caledonia; Chevalier et al., 2015b), whereas in large coral-reef lagoons water transits mostly through passages (e.g., Noumea located few kilometers southward Ouano; Ouillon et al., 2010). The tidal propagation plays also a determinant role in the lagoon hydrodynamics functioning. For instance, with propagating tidal wave the cross-reef flow can be low and sometimes even outflow as in Mayotte lagoon (Chevalier et al, 2017), whereas with a stationary tidal wave, it can be much more important as in Toliara lagoon located in the same geographical area and having a similar geomorphology as Mayotte (Chevalier et al, 2015a). Influence of other factors, such as wind, has been observed to be often much less significant. It seems more likely that, when moderate, near the reef, the wind affects the incident wave energy, mainly as energy from a short wind fetch and can often be neglected (Kench and Mclean, 2004; Lowe et al., 2009, Chevalier et al., 2015a).

This paper investigates the links between swell, tide and cross-reef flow in channel lagoons. Taking the Toliara Great Reef Lagoon lagoon (GRT) in Madagascar as an example, it examines the coupling effects of wave and tide on cross-reef flow and lagoon water renewal by means of numerical circulation modelling, in order to accurately estimate the relative importance of these two main forcing in different tidal amplitude and wave height conditions. This article is divided into three parts. After describing the study site, the model and data set used to validate and calibrate the model will be presented. The circulation patterns and water age from September to December 2008 will be described. Then, the results of the hydrodynamic model and water age computation will be discussed to assess how wave and tide modulate circulation and water renewal.

I. Methodology

II.1- Study field

a. Description

The Great Reef of Toliara (GRT) is a channel lagoon located on the south-western side of the island of Madagascar (23°25' S and 43°40' E), bounded to the east by the city of Toliara (Figure 1). The lagoon is approximately 20 km long and extends between the mouths of the rivers of Fiherenana in the north-east and Onilahy in the south-east. The lagoon is partially separated from the Mozambique Channel by the largest coral reef in Madagascar (approximately 18 km long and 1.5 to 4 km wide, Andréfouët et al., 2013) which is immersed at high water and partially or totally emerged at low water. Its width ranges from 2 km in the south to 10 km in the middle and it is open to the ocean via two passages along the coast, to the north and to the south. The northern passage (NP) is 2km wide with an average depth of about 21 m, while the southern passage (SP) is 4 km wide with a depth of about 10m (Chevalier et al, 2015a). The SP is characterized by the presence of a reef block (Nosy Tofara) which divides it into two sub-passages: the wide southern passage (WSP) and the narrow southern passage (NSP), of 2.55 km and 0.45 km width, respectively, the mean depth is about 9 m. Along the coast, the Toliara bay and the Belaze bay are very shallow (less than 5 m) and could emerge partially. Depth outside the southern part of the reef increases abruptly, reaching 100m at a distance of 1 km from the reef flat and 1025 m at a distance of 2 km from the southern end (Battistini et al, 1975).

The mean coastal current observed off the lagoon is mostly northward (Chevalier et al, 2015a). It is driven by a semi-diurnal tide with an amplitude ranging from 0.8 to 3 m (Chevalier et al. 2015a). Furthermore, ocean swell, with a significant wave height reaching 1.64 m during the rainy season (December to March) and 3.5 m during the dry season (April to November), breaks along the reef barrier and induces a high inflow above the reef. The south-west trade winds blow during the rainy season, whereas the south-east trade winds blow during the cool season. According to Chevalier et al (2015a), the influence of these winds on the lagoon circulation patterns is low, but the cyclones which sometimes occur in the area may modulate the lagoon's circulation pattern.

a. In-situ Data

Acoustic Doppler Current Profilers (ADCP) moorings (Figure 1) were deployed during three field campaigns carried out at the Toliara lagoon in the frame of the project Impact of Climate and Anthropogenic Changes on trophic flux of Toliara Great Reef (ICAR-GRT; 2007-2008). During the first campaign (C1, from August 23 to October 13, 2007), four ADPC were moored: two in the southern passage (moorings S1 and S2); one in the northern passage (mooring N) and the fourth in the middle lagoon (mooring M). During the second campaign (C2, from March 3 to

April 4, 2008), as during the first campaign, three ADCP were deployed in the SP and NP (mooring S1', S2' and N'). Finally, during the third campaign (C3; October 20 - November 27, 2008), only one ADCP was moored on the northern part of the reef barrier (mooring B). These moorings recorded measurements of currents and water levels at each station, except at mooring M which provided only measurement of current. These data are used for calibration and validation of the model. To use independent data to validate the model and avoid overlap, C1 and C3 data are used to fit model parameters as drag coefficient and cross-reef flows, whereas C2 data are used to validate simulations. Campaign description and device characteristics are detailed in Chevalier et al. (2015a).

b. Statistical fit indices

Following Liu et al. (2009), two statistical indices are used to evaluate and quantify the fit of the model to data. The Root Mean Square Error (RMSE) gives the quantitative difference between the measured and modelled change. The skill factor (equation 1; Willmott, 1981) which has been used by many investigators in assessing coastal ocean circulation models (Liu et al., 2009) captures the fit between the measured and modelled data. The highest value, skill factor = 1, means perfect agreement modeled and measured values, whereas the lowest value, 0, indicates complete disagreement.

$$Skill = 1 - \frac{\sum_{i=0}^{N} |X_{mod}(t_i) - X_{obs}(t_i)|^2}{\sum_{i=0}^{N} (|X_{mod}(t_i) - \overline{X_{obs}}| + |X_{obs}(t_i) - \overline{X_{obs}}|)^2} \quad (1)$$

Where $X_{mod}(t_i)$ is the predicted value, $X_{obs}(t_i)$ is the measured value N is the number of time step; the top bar means the average value for the series.

II.3. Hydrodynamic model

a. Description and numerical choices

Model description:

The numerical model used for this study was the Coastal and Regional Ocean Community (CROCO). This recent non-hydrostatic three-dimensional numerical model is based on ROMS-AGRIF model (Penven et al., 2006). CROCO is a free surface, primitive equation model that solves finite-difference approximations of the Reynolds averaged Navier–Stokes. It uses a horizontal orthogonal Arakawa C, with a splitting stepping algorithm (Haidvogel et al., 2008). Our configurations were run with Large-McWilliams-Doney interior closure scheme with the K-profile parametrization (KPP) (Large et al., 1994) for the vertical turbulence closure scheme.

Boundary conditions

In the Toliara configuration, the grid is rectangular with two open boundaries at the western and northern boundaries (Figure 1). The amplitude and phases of the tide are specified at the western boundary, whereas Chapman condition (Chapman, 1985) constrains water surface elevation at the northern boundary. The barotropic velocity is deduced from Neuman condition (with velocity gradient set to zero) and the 3D velocity is driven by the adaptive radiation scheme of Marchesiello et al. (2001).

In wind conditions such as those observed during our measurement campaigns, the direct influence of the wind on the cross-reef current can be neglected, as it was in other lagoon studies (Kench and Mclean, 2004; Lowe et al., 2009) where wind conditions were similar. It seemed more likely that, near the reef, the wind affected the incident wave energy, mainly as energy from a short wind fetch.

Grid and bathymetry

The grid system is inclined 30° with the north towards a north-north-west direction, in order to follow the orientation of the lagoon coastline. The model is run on a 100m horizontal resolution grid (333x158 mesh), with 9 sigma vertical layers. Realistic bathymetry (Figure 1) was extracted from the SHOM (*Service hydrographique et océanographique*

de la marine) digital elevation model of 2006. Over the model grid, interpolation and smoothing use the Shapiro filter.

The barotropic time step is set to 1s to respect the Current of -Friedrich Levy (CFL), whereas the baroclinic time step is set to 10s. For more model stability, the wet and dry function was applied to remove all mesh where water depth is less than 0.02 m.

b. Bottom friction

The bottom boundary conditions are "slip conditions" with friction in the deepest layer (Blumberg and Mellor, 1987; Deleersnijder, 1992). Bottom stress is parameterized through a quadratic function of velocity representing a logarithmic layer adjacent to the bottom (Blumberg and Mellor, 1987; Deleersnijder, 1992). The bottom friction is computed from the quadratic linear law (equation 3) that depends on horizontal velocity, U_b, at the bottom adjacent mesh, the water density ρ, and the bottom drag coefficient, C_d (Blumberg and Mellor, 1987).

$$\vec{\tau}_b = \rho C_d \left\| \vec{U}_b \right\| \vec{U}_b \qquad (2)$$

To take into account the variability of the bottom nature in the drag coefficient, we implemented a spatially variable roughness in the model, according to the type and nature of sediments (silts, sand, corals, etc.). The area is separated into three zones with different characteristics:

- The foreshore zone mainly governed by the wet and dry effects and composed of fine sand (Blanchot personal communication); this area is characterized by flow bottom friction. The coefficient is set to C_d = 0.0035;

- The sandy lagoon area between the foreshore zone and reef barrier and outside the lagoon; The drag coefficient is set to a standard value as suggested by Blumberg and Mellor (1987): C_d = 0.0025 ;

- The reef is often characterized by abnormally strong friction due to the bottom roughness (Monismith 2007); the drag coefficient is set to C_d = 0.02, in agreement with studies in other lagoons (Mayotte and Ouano lagoons; Chevalier et al., (2015b), (2017)) and reef systems (Hearn, 1999)

With these bottom drag coefficients, the skill factor is above 0.97 for water level and above 0.93 for velocities during campaigns.

c. Cross-reef flow:

Wave breaking on the reef slope generates cross-reef flow which were measured in 2008 (Chevalier et al, 2015a). This transport is driven by cross-shore spatial gradients in radiation stresses. As suggested by some authors (Longuet-Higgins and Stewart,1964; Symonds et al., 1995; Gourlay and Colleter, 2005; Monismith et al., 2013), the energy transfer from the swell breaking to the current is introduced with the radiation stress on the reef barrier in the model:

$$\begin{cases} F_x = \frac{-1}{\rho}\left(\frac{\delta S_{(xx)}}{\delta x} + \frac{\delta S_{(xy)}}{\delta y}\right) \\ F_y = \frac{-1}{\rho}\left(\frac{\delta S_{(yx)}}{\delta x} + \frac{\delta S_{(yy)}}{\delta y}\right) \end{cases} \qquad (3)$$

With, F_x and F_y being the radiation stress along the cross-shore and alongshore direction; S_{xx} and S_{yy} corresponds to the excess of the amount of movement brought by the waves through a plane x and y constant respectively. The term S_{xy} and S_{yx} can be interpreted as the flow of momentum according to x through the plane y constant.

The significant wave height (Hs) of swell during campaigns comes from the open-access dataset of WaveWatch III (WW3) model (Tolman, 2006) which offers higher spatial (0.5 x 0.5°) and temporal resolution (8 measurements a day). However, the model resolution rules out taking into account the deformation of the swell when it arrives on the reef. To overcome this and avoid the problem of local turbulence variability due to coral specificity, the radiation stress components are parameterized above the reef to fit with in-situ velocity data. Assuming the radiation stress above the reef is mainly cross-reef, only the cross-reef component of radiation stress, F_x is parametrized. Moreover, we suppose it is only dependent on swell and water depth. Due the lack of data, we consider it as constant all along the barrier reef. On the basis of these assumptions and using the C3 data, we estimate F_x as:

$$\begin{cases} F_x = -22.10^{-4}Hs + 19.10^{-4} & \text{if } Hs < Hc \\ F_x = -46.10^{-4}Hs + 48.10^{-4} & \text{if } Hs > Hc \end{cases} \quad (4)$$

With:

Hc : the cutoff height of the two functions, $Hc = 1.22\ m$

The outputs of the model with the radiation stress well represent the main features of the temporal patterns of the observations (Figure 2). Our model configuration has a skill factor of 0.95 with C3 campaign data time series of cross-reef flow. This high skill factor (Table 1) reveals the model's ability to simulate the tidal high-frequency cross-reef flow variations in relation with wave changes or spring and neap tide variations.

For wave height under 1.22 m, the model smooths out the temporal variability of the flow. However, it is qualitatively and quantitatively in agreement with the data with a skill factor above 0.95. The model better represents the observed flow than the parametrized function suggested by Chevalier et al (2015a), especially during high wave conditions events (October 27 and November 20, 2008) and in neap tides (results not shown here). This improvement is also apparent in the correlation between the modelled and the in-situ cross-reef flow: the correlation was 0.72 with the parametrized function and increases to 0.91 with configuration by radiation stress.

d. Validation

In order to calibrate and validate the model, numerical data are compared both qualitatively and quantitatively with in-situ data. For tidal components, harmonic constants of water level and velocity fluctuation are compared with those derived from in-situ data, whereas the statistical indices evaluate the correspondence of the model to data in the entirety of the signal.

As observed by field measurements (Chevalier et al, 2015a), the lagoon hydrodynamics is affected by in-flowing or out-flowing cross-reef flows induced both by the tide and by the waves breaking on the reef. The numerical model reproduces this aspect (Figure 3). Velocity and water level are generally well estimated by the model (skill factor higher than 0.98), even though the amplitude of the highest and lowest peaks may be under-estimated or over-estimated mainly during the neap tide period (Figure 4). The differences between modelled and observed tidal harmonics components (phase and amplitude) at the ADCP locations are also provided in Table 2. The deviations are lower than 11% and 1.5 degrees respectively at all of the tidal gauges except at station S2, where the phase is more than 5 degrees higher in the data. This relative high lag would be primarily attributable to the presence of a coral reef block between the WSP and NSP passages. This obstacle leads to the dispersion of the incoming and outgoing flows of lagoon and also to the dissipation of tidal energy caused either by the narrowness or by the shallowness of the NSP passage. It is also very important to note that slight local depth changes do not significantly affect modelled water surface elevations in the lagoon zone.

As shown in Table 1, the skill factor is higher than 0.95 for the long-shore component and above 0.93 for the cross-shore component. Therefore, we can conclude that the model is consistent with the data qualitatively and quantitatively, even if we can note a slight increase of errors during higher wave conditions. The use of radiation stress to model the cross-reef flow is effective in reproducing temporal circulation trends in the whole lagoon and improves the agreement between the model and the observations.

II.4. Modelling water age and water origin

To characterize the lagoon renewal dynamics and the lagoon ecological functioning, a focus is made on the age and origin of the water calculated with the Constituent-oriented Age and Residence time Theory (Deleersnijder and Delhez, E. J. M., 2006, Delhez et al. 1999; Gourgue et al., 2007; de Bry et al., 2013). These relevant quantities integrate the dynamics and history of lagoon waters (Delhez and Deleersnijder, 2002). For instance, as defined by De Brye et al., (2013) "the age of a water parcel located at point x and time t is the time elapsed since the water parcel entered the domain of interest", whereas the origin indicates where the parcel come from. These quantities have been revealed to be good indicators of water quality in coastal areas such as lagoons (Chevalier et al., 2017) and estuaries (Karna and Baptista, 2016) and to well-suit the exploration of predator-prey dynamics and matter fluxes in aquatic ecosystems (Deleersnijder and Delhez, 2006).

Though these concepts are Lagrangian concepts, they can be estimated from a Eulerian approach (Delhez et al., 2014) as described in De Brye et al. (2013). The age is calculated inside the lagoon and the external domain is divided in three areas: (i) the reef area which covers the surface of the reef, (ii) the NP and (iii) the SP. Then, this method allows to determine both age of lagoon water and the way the water use to enter inside the lagoon. For each simulation, when constant forcing (waves and tides) is applied, the computation of age and origin of lagoon water shows an asymptotic behaviour. The simulations are thus set to last until all lagoon water is renewed (until few hundred days for some simulation cases) and asymptotic values reached by both age and origin are extracted and analysed.

II.5. Sets of simulations

Three sets of simulations (Table 3a) with 135 simulations have been performed:

- ***3 realistic simulations*** to describe and analyze the dynamics inside the lagoon. The two main harmonics (amplitude and phase) components of the solar (S_2, 12 hours) and lunar (M_2, 12.42 hours) semi-diurnal tide represent more than 95% of the tidal signal (Chevalier et al., 2015). Then, to reduce forcing variability and to better understand spring and neap tide influences, simulations only take into account these two tidal components. These simulations take also into account the significant wave height of the ww3 model ranging from 0.69 m to 3.45 m. Simulations are performed from the three field measurement periods (C1, C2, C3) and the spin-up is estimated to last about twenty days. Instantaneous model results (water surface level and velocity) were recorded hourly.

- ***125 sensitivity simulations*** to understand the respective influence of these forcings. In these simulations, significant wave height and tidal amplitude were assumed to be constant (Table 3b). Significant wave height ranges from 0 m to 3 m and tide from 0.3 m to 1.5 m, with a period of 12.42 hours corresponding to the M_2 tide component. Simulations last 30 days.

- ***7 semi-realistic simulations*** to evaluate the time lag of the system response. 3 simulations with constant semi-diurnal tide (with tidal amplitude set to 0.3, 0.8, 1.2 m) and realistic wave (significant wave height ranging from 0.64 and 3.5 m) and 4 simulations with constant wave height (with 4 different significant wave height set to 0.3; 0.85; 1 and 1.2 m) and a realistic tide (tidal amplitude ranging from 0.3 m at neap tide to 1.5 m at spring tide).

III. Results

III.1 Hydrodynamic characteristics of the GRT

The circulation in the GRT was studied during the three field campaign periods. The water level fluctuation amplitude ranges from 1.2 m during spring tide to 0.3 m during neap tide. The swell breaking above the reef ranges from 0.6 m to 3 m. For instance, from September 1 to November 27, 2008 (Figure 5), the realistic model presents 8 spring tides and 8 neap tides. The swell ranges from 0.69 m to 3 m. Six events of high wave conditions (significant wave height higher than 2 m) may be noted: namely September from 3 to 8 and December 26 with waves reaching 2.7 m (Figure 5), whereas 4 events during low wave conditions (significant wave height under 1 m) are modelled.

Therefore, we observe spring tide with low waves conditions (significant wave height of about 0.6 m) on September 16, or conversely neap tide with high wave conditions (significant wave height above 2 m) on November 19.

Outside the lagoon, vortex structures arise in Saint-Agustin bay during the ebb and flood phases (Figure 3). These small-scale structures result from the SP (WSP and NSP) jet induced by the lagoon tidal emptying and which run into the tidal current flowing along the southern coast of Saint-Agustin bay. They are also reinforced by the geomorphology of the Sarodrano bay headland which redirects the current northward.

Inside the lagoon (Figure 3), the dynamics are determined by the flows through the passages and above the reef. The tide is almost stationary, and the sea level is in quadrature with tidal velocities. Through passages, water enters and leaves the lagoon with the flood and ebb currents. The cross-reef flow is mainly inwards. It increases just before the flood, is at a maximum at the end of the flood (reaching 0.3 $m.s^{-1}$ for a mean tide (tidal amplitude of 1 m) and a mean wave height (significant wave height of 2 m) and begins to decrease at the end of the flood. It is slow during high water and can be reversed during the ebb. However, cross-reef flow is also strongly modulated by swell breaking over the reef, mainly causing inflows. Hence, the tidally-averaged cross-reef flow increases when the swell is high (for example, during periods October from 24 to 26, and November 20 to 22, 2008, Figure 2; Figure 6a and b) whereas it decreases during low wave conditions (November 1 to 4, 2008, and November 15 to 17, Figure 2; Figure 6c and d,). In agreement with the mass conservation law, this induces respectively an increase and a decrease of the tidally averaged outflow through the passage (Figure 6) and deeply modifies the tidal lagoon dynamics (Figure 6). For example, whereas during low wave conditions and spring tide (Figure 6 c and d), the circulation is mainly driven by the flux entering the lagoon through the two passages and spreading inside the lagoon from the north and from the south, we can observe (Figure 6a,b), that with 0.6 m of tidal amplitude (neap tide), high wave breaking on the reef modified the circulation inside the lagoon The velocity through the passages is weaker and a north-south circulation pattern along the coast occurs in order to fill Belaze bay.

Currents are strongest during flood and ebb, with maximum intensities (reaching about 0.23 to 0.35 $m.s^{-1}$) in spring tide periods (Figure 6 (c) and (d)), while they weaken during slack water when the current reverses (Figure 3 (b) and (d)), as a classical standing wave. Maximum velocities mainly occur in the two southern passages (WSP and NSP, with values up to 0.3 $m.s^{-1}$), above the reef and in Belaze Bay too. This bay is characterized by strong bathymetry gradients and reef inlets that induce local hydraulic effects where the current intensity is amplified.

Above the reef (depth less than 5 m), the west-east direction (cross-shore) current dominates, while in the middle of the lagoon, currents are mainly in the north-south direction (along-shore). In the northern part of the lagoon, between latitudes 23.38° S and 23.45° S we can observe an area where velocities diverge during the ebb and converge during the flood. South of this front, the current is northwards the north during the flood whereas it is southward during the ebb (Figure 3). North of the front, the situation is reversed. This front has already been anticipated by Chevalier et al. (2015) as an anti-node of a standing wave. It is also important to note that during event of neap tide, and high wave conditions, the flux through the lagoon passes is almost always outgoing (Figure 6).

Furthermore, due to the tidal amplitude, shallow water area at high tide emerges at low water. Hence, the immersed coastline may vary drastically along the tidal cycle, namely during spring tide. Thus, we observe a change of the direction of local currents in relation with this immersed coastline tidal change. For instance, the coral reef and very shallow areas (Sarodrano reef, Belaze Bays) emerge partially or sometimes totally during low water and during low wave conditions, which induces a velocity increase. For instance, on November 8, 2008 at 20h (Figure 3 (d)) with a significant wave height of 1.5 m and a tidal amplitude of 2 m, the coral reefs in the vicinity of the Killibé and Microbe channels (Belaze bay) and the part of the coral block separating WSP and NSP emerged during low water, and canalized the circulation increasing the velocity in the passage (Figure 3d versus Figure 3b).

III.2. Water origin

During the simulated periods, about 55% (from 20% to 80%, during the third campaign) of water inside the lagoon is advected by cross-reef flow (here after called "cross-reef water"), whereas about 45% of the lagoon water transits through passages (here after called "through-passages water"). However, this origin is subject to spatial (Figure 7a)

and temporal (Figure 5.c) variability. As expected, near the reef, water comes from cross-reef flow, whereas the water near the passages mainly comes from the opening close to its location. Due to the channel cross-section dimensions, the amount of water having transited from SP is higher than that having transited from NP which is confined only in the northern area of the lagoon. The water coming from the south spread in the south of the lagoon, and a part is advected towards Toliara bay where the water tends to remain. This distribution pattern also varies during the tidal cycle with more through-passages water during high water than during low water and cross-reef flow water remaining quite steady. However, the proportion of cross-reef water varies with swell height (figure 8a and b). It increases to 80% during high wave conditions and neap tides (November from 19 to 20, Figure 5), whereas the quantity of through-passages water increases during the spring tide, with a maximum (80%) during the end of the spring tide, and low wave conditions (September 16, 2008, for instance,). During low wave conditions, the cross-reef water is confined to the middle of the lagoon near the current front observed previously (figure 8b). In contrast, it is spread throughout the lagoon during high wave conditions (figure 8a) and reaches Belaze bay near the passage.

III.3. Age of water

The temporal changes of mean water age are shown in Figure 5d. The mean lagoon water age ranges from about 1 (September 16) to 3 days (November 3). Spatially, water age ranged between 0.25 and 5 days in the lagoon area (Figure 7b). In the shallow water Belaze and Sarodrano bays, the water age is often higher, revealing an area protected from water exchange by the cape and by shallow water. In the main part of the lagoon, the water age is under 3 days. In the vicinity of the passages and the reef barrier the water age is low: under 1 day on average and varying over the tidal cycle: it is lower at high water and higher at low water.

Furthermore, water age varies with ocean/lagoon exchange intensity (Figure 5 and Figure 8c and d). Water age below 1 day are observed at different periods (September 14, October 27 and December 28) characterized by a spring tide and close to an event during high wave conditions (about 1 day after), and higher water age (about 3 days) are observed at six other periods (e.g. November 17) close to neap tide and enhanced 1 or 2 days after an event of wave under 1.2 m. Hence, when waves are high, the water age tends to decrease, and vice-versa. However, when ocean/lagoon tidal exchanges are intensified during the spring tide, the water age also tends to decrease (for instance, on 13-16 November).

During high wave conditions and neap tide (Figure 8b), the water comes from the reef and pushes lagoon water towards the coast, inducing a through passage outflow. The lagoon water is then renewed, except near Belaze bay where through-passage water is constrained by the cross-reef water and Sarodrano cape. Then, water in Belaze bay is very slowly renewed until the tidal wave increases. In contrast, when the swell is weak and the tide is high (Figure 8d), the tide pushes water into the current front area, near Toliara bay, where the renewal is slow. Hence, the water age in this front area increases during low wave conditions, whereas the mean water age decreases in the whole lagoon.

More precisely, the cross-reef water is younger than the through-passages water (1 day versus 5 days on average, results not shown).

IV. DISCUSSION

The realistic simulations highlight the main roles of waves and tides in the dynamics of water masses in the lagoon. Their strong variations have important consequences with regard to the fluxes of materials exchanged between the lagoon and the ocean as well as to the enrichment of reef corals (Atkinson and Coleman, 1992). These simulations highlight the coupled effect of tide and swell on the ocean-lagoon exchange and on dynamic processes in the lagoon-reef system. Realistic simulations show that (1) the cross-reef inflow and the through-passages outflow increased during high wave conditions; whereas during low wave conditions the through-passages outflow and the cross-reef inflow decrease during spring tide, with even a temporary outflow as observed on November 1 - 3; (2) the proportion of cross-reef water decreases a few days after spring tide. In opposite, it increases a few days after neap tide; this tendency may be reinforced by wave (3) water age is linked to the wave and tide influence, but the link is less clear.

IV.1 Effect of swell vs. tide on ocean-lagoon water exchanges

The cross-reef inflows are directly correlated to the significant wave height (r= 0.88) and, to compensate this water arrival, the through-passage flow is outwards and also correlated with the significant wave height. In the same way, the tide modulates these flows: spring tides generate higher flows than neap tides. These results corroborate quite well those of Chevalier et al. (2015b, 2017) on the circulation in the Ouano and Mayotte channel lagoons studied under the same conditions and with local data, or those of Bonneton et al. (2007) on the Noumea lagoon based on experimental observations. However, tide and wave forcing are intrinsically mixed. In order to separate them, we used forced sensitivity simulations with idealized wave and tide data. To better understand the respective influences of the wave height and the tidal amplitude on the lagoon water exchange, we analyzed the flows in function of constant wave height and constant tidal amplitude (Figure 9).

- When wave height is below 0.85 m, average cross-reef flow is outflow whatever the tidal amplitude (Figure 9). These situations are characterized by the absence of swell breaking over the reef flat. Consequently, tidal currents are the main driving force of the circulation in the lagoon, which is essentially supplied (flood) and emptied (ebb) of water through passages. The intensity of these flows increases with, tidal amplitude but decrease with wave height. This is what happened in realistic simulations on September 16 during flood and ebb (Figure 6c and d).

- When waves have a height greater than 0.85 m, cross-reef inflow occurs. Through-passages outflows balance the instantaneous pressure gradient in the lagoon-ocean system, as observed in the realistic situations on November 20 (Figure 6a, b). The intensity of these flows increases with wave height, but also with tidal amplitude. Hence, with a tidal amplitude of about 0.8 m and a significant wave height of 2 m, cross-reef flows are the same as those with a tidal amplitude of about 1.5 m and a significant wave height of 1.5 m (Figure 9).

Therefore, these results highlight the opposing effects of tide on the tidally averaged fluxes depending on the wave size: whereas during small wave conditions, increasing tidal amplitude or decreasing wave height induces a mean cross-reef outflow increase; during higher wave conditions, the cross-reef inflow increases with tidal amplitude increase. The tidally averaged cross-reef inflows also increase with significant wave height during high wave conditions, but when the wave is low, no breaking can occur, and the wave forcing is weak and wave reduce the cross-reef outflow.

IV.2. Effect of swell vs. tide on the age and origin of the lagoon water

The effect of tide and wave on the origin and age of lagoon water is also analyzed by means of the schematic experiments. The mean water age and the mean proportion of cross-reef water are determined for each configuration with a constant wave and a constant tidal amplitude (Figure 10).

As expected (IV.1), the part of cross-reef water increases with the wave height and decreases when the tidal amplitude increases. However, as for the cross-reef flow, there is a threshold and we observe a split around a wave height of 0.85 m. Below this threshold, the part of cross-reef water is quite constant, from 0 to 10%. Above a wave height of 1.2 m, this part is more than 70%. It increases with wave height and, contrary to the cross-reef flow (IV.1), it decreases with increasing tidal amplitude. Between 0.85 m and 1.2 m, the wave influence is predominant, and the cross-reef water proportion varies from 10% to 70%, mainly in relation with wave height since the tidal amplitude influence is low.

The variation of the water age seems to be much more complex. The mean water age ranges from about 0 to about 4 days. It decreases with tidal amplitude, but the wave influence is less consistent. As before, a threshold is observed when the wave height reaches 0.85 m. For any given tidal amplitude, the mean water age is highest at this threshold. Therefore, as expected, the maximum water age values are observed for a low tidal amplitude and a wave of about 0.85 m.

- Below the threshold of 0.85 m wave height, the tide is the main forcing with about 95% of through-passage water (78% through SP and 17% through NP). The water age decreases with the tide and increases with wave

height. The water is renewed with the succession of flood and ebb, pushing old water into the middle of lagoon until it flows out of the lagoon above the reef (figure 8d). The oldest water is observed along the coast. During low wave conditions, cross-reef outflow is limited by waves which break along the reef and reduce ocean-lagoon exchange. Thus, the water age increases with wave height and the minimum water age (about 2 days) is obtained for smaller waves and a tidal amplitude of 0.4 m which prevent breaking waves (Figure 8 b and d), whereas the maximum water age is reached for a 0.85 m significant wave height and smaller tidal amplitude.

During realistic simulations, low wave conditions (significant wave height under 0.85 m) occur very rarely (on September 20, October 10, November 2 and December 1), but its influence on the water age is not clear (Figure 5) in relation with the too short duration of this event.

- Above the wave threshold of 0.85 m, wave and tide have an influence on the water age similar to their influence on the lagoon-ocean exchange intensity. Cross-reef flow is predominant in the renewal process. It pushes the water into the middle of lagoon where the strong mid-lagoon current exports it outside the lagoon (Figure 6). Hence, the water in the lagoon is mainly advected by cross-reef flow and the age of the water decreases when the wave height increases. The bay, protected against the cross-reef influence, keeps the oldest water. A similar process can be observed on October 27 and November 2 (Figure 8 a and d).

These results corroborate those of Chevalier et al. (2015b) on Ouano lagoon where 85% of the lagoon water originated from cross-reef with high waves, while in Mayotte the proportion of cross-reef water was 43% with moderate waves.

IV.3 Phase lag between tidal or wave variation and age (or origin) of water

Realistic simulations are in agreement with these previous schematic tests, and the age and origin of the water vary with tidal amplitude and wave height. However, we can observe that their variations do not occur simultaneously. The decrease of wave height observed on October 22 seems to induce an increase of water age five days later (i.e., on October 27; Figure 8). In the same way, we observed an increase of the part of the through-passage water a few days after the spring tide. To analyze the time lags, two sets of numerical experiments were conducted.

Firstly, with a constant tidal amplitude, the wave height changes according to the realistic simulation. In correlation with realistic simulations, we observed a phase lag between the event and the response to this event. The change of water origin occurs between 5 and 8 days after the decrease of wave height. Furthermore, this phase lag increases with the tidal amplitude: for instance, the low wave conditions event of the October 22 seems to induce a decrease of the part of the cross-reef water nine days later (October 31) for a tidal amplitude of 0.3 m and four days later (October 26) for a higher tidal amplitude. The phase lag is also modulated by the wave and its variability during the latency period. Therefore, for the low wave conditions event of November 2, 2008, the corresponding decrease of the part of the cross-reef water seems to occur seven days later (November 9) for 1.2 m of tidal amplitude or 9 days later (November 11), for a tidal amplitude of 0.3 m.

Water age increases rapidly after the decrease of cross-reef water (Figure 11) and it reaches its maximum less than one day after the minimum of cross-reef water proportion. Therefore, the water age increase occurs between 5 and 8 days after the decrease of wave height and is modulated by the tidal amplitude and by the wave variability during the latency period. For instance, the low wave conditions event of November 2, 2008 (significant wave height of about 0.6 m), induces an increase of water age on November 9, 2008 for tidal amplitude of 1.2 m or on November 11, for a tidal amplitude of 0.3 m whereas that of October 22 induces a water age increase on October 26 and 31, respectively.

The second set of experiments is with a constant wave height and a fortnightly modulation of the tidal amplitude. They highlight that the maximum of through-passages water occurs a few days after the spring tide (Figure 12). The time lag between the tide increase and the increase of the proportion of through-passages water is low during high wave conditions and increases when the wave decreases. For instance, the spring tide of November 12 induces a

maximum part of through-passages water on November 12 and 14 for a wave height of 1.2 m and 1 m, respectively. This appears during neap tide, on November 18-19 for a wave below the threshold of 0.85 m.

As previously, a threshold of 0.85 m wave height is apparent. Below this threshold, the tide, the part of cross-reef water and the water age fluctuate in quite opposite phases with a time lag of 1 or 2 days, whereas above this threshold they seem to fluctuate together with a small time lag. In the same way, the time lag depends on the wave height. The maximum of water age is reached on November 20, just after the neap tide (November 18) and during low wave conditions (with significant wave height of 0.3 and 0.85 m), whereas it occurs, on November 18 and 16, just before the neap tide during high wave conditions (with significant wave height of 1 and 1.2 m, respectively).

V. CONCLUSIONS AND PERSPECTIVES

In this article, based on a case study of the Toliara channel lagoon in Madagascar, we have identified the impact of the main drivers (namely tide and breaking waves) on the hydrodynamics of typical channel lagoons. For this purpose, a hydrodynamics numerical model of circulation patterns was implemented in 2007 and 2008.

This study highlights the coupled effect of tide and waves on the ocean-lagoon exchanges: (i) during low wave conditions (significant wave height <0.85 m), tide and waves have antagonistic actions, with waves increasing the cross-reef inflow and tide favoring the cross-reef outflows with ocean-lagoon exchange being at a minimum when wave and tide action neutralize each other (i.e. with 0.85 m wave height and 0.3 m tidal amplitude); (ii) during higher wave conditions, as soon as a wave is above the threshold, both tide and wave increase ocean-lagoon exchanges, with swell breaking driving water above the reef thus increasing cross-reef inflow and favoring through-passage outflow. Tide also accentuates these exchanges by reinforcing the wave action on the cross-reef inflow. Water mass inputs and their trajectory depend not only on the amplitude of the tide, but also on the height of the incident ocean swell that actually varies during the period of large-scale atmospheric disturbances and variations in water depth above the reef. Strong variations of waves and tides would have important consequences for the fluxes of materials exchanged between the lagoon and the ocean and consequently for the ecological functioning of the reefs and the lagoons. For example, these processes impact the enrichment of reef corals which draw their nutrients from reef waters (Atkinson et al, 2001). Besides, cross-reef and through-passage waters having not the same characteristics, their relative contribution to the water balance may result in selective plankton exchanges between the lagoon, and the ocean leading to plankton retention in the lagoon partly explaining the high productivity of these coral reef ecosystems compared to the surrounding ocean (Pagano et al., 2017).

Our results also highlight the importance of tide and swell for lagoon water renewal: (i) below a significant wave height of 0.85 m, the cross-reef flow tends to be outflow, there is less water renewal when the wave increases (remaining below 0.85 m) and tidal induced renewal is mainly due to through-passages flows; (ii) during higher wave conditions (above the threshold of 0.85), a significant amount of water enters the lagoon through the reef and exits through the passages, and the water age decreases with tide and wave height and the main part of the water entering the lagoon is cross-reef water. However, in real configurations, the tide and wave influences are not immediate, and a time lag occurs between wave, tide and water age (or origin) and this time lag varies with tide and wave and needs to be studied further. These processes may also have great importance for the ecological traits of the lagoons, since water renewal directly impacts the phytoplankton stock in coral reef lagoons (Delassale and Sournia, 1992) and this effect seems to be particularly high in channel lagoons as suggested by Chevalier et al. (2017).

Figure 1 : Location of the Toliara GRT lagoon zone (Madagascar) : The black line shows isolines of the bathymetry in meters (m). The lagoon passages are noted as follows: northern passage (NP) and southern passage (SP) which is divided into the wider southern passage (WSP; to the east) and the narrower southern passage (NSP; to the west), and lastly the reef (B). The ADCPs (WSP, NSP and NP) moorings are shown by: First campaign (C1, red squares); second campaign (C2, red circles); third campaign (C3, red triangles); the names of these moorings (see text) are given in red characters.

Figure 2 : Comparison between model results (red) and field measurement over the reef barrier during the C3 campaign (October 20, 2008 - November 28, 2008). (a) Water Level; (b) Tidally averaged of vertical integrated flow; (c) Vertical integrated flow.

Figure 3 : Spatial distribution of the instantaneous surface direction (arrows) and intensity (colorbar) current velocities obtained by CROCO model the November 8 – 9 characterized by a tide with mean amplitude (1 m) and external swell with mean significant wave height of about 1.45 m. (a) at 17:00, the 8 (mid-point of the flood), (b) at 20h, the 8 (high water), (c) at 23h, the 8 (mid-point of ebb) and (d) at 2 h, the 9 (low water).

Figure 4 : Comparison between model results (red) and field measurements (black) during Campaign 1 (a) and Campaign 2 (b). Water level in NP (top), Velocity in the main current direction in NSP (bottom).

Figure 5 : Time series of (a) water level, (b) wave height, (c) percent of cross-reef water and (d) global mean water age over the lagoon area between September 1, 2008 and December 31, 2008.

Figure 6 : Spatial distribution of the instantaneous surface direction (arrows) and intensity (colorbar) current velocities obtained by CROCO model :

During neap tide (on November 19-20, 2008) with a tidal amplitude of about 0.7 m and during high wave conditions (wave of about 2 m height): (a) during the flood (November 20, 2008, 00:00) (b) during the ebb (November 19, 2008 at 17h)

During spring tide phase (September 16, 2008) with about 1.4 m tidal amplitude and during low wave conditions (wave height of about 0.6 m) at flood (08:00) (c) and at ebb (14:00) (d).

Figure 7 : Spatial distribution of (a) the average (from September 1, 2008 to December 31, 2008) of the part advected by cross-reef flow and (b) the mean water age.

Figure 8 : Spatial distribution of instantaneous variability of ratio of reef water in the lagoon (a and b) and water age (c and d) : November 19, 2008, 17h – neap tide and high wave conditions (a and c) and September 16, 2008, 14h – spring tide – low wave conditions (b and d) .

Figure 9 : Variability of lagoon/ocean water flow (through-passage outflow or cross-reef inflow) in function of wave height for a tide of 1.2 m (a) and versus wave height and tide amplitude (b).

Figure 10 : Variability of mean water age (a) and percent of reef water (b) in the lagoon versus wave height and tide amplitude.

Figure 11 : Time series of wave height (a), mean age and reef water percent in the lagoon for constant tide amplitude (0.3 m (b), 0.8 m (c) and 1.2 m (d)).

Figure 12 : Time series of tide amplitude (a), mean age and reef water percent in the lagoon for constant wave height (0.3 m (b), 0.88 m (c), 1 m (d) and 1.2 m (e)).

Refererences:

Andréfouët, S., Pages, J., Tartinville, B., 2001. Water renewal time for classification of atoll lagoons in the tuamotu archipelago (french polynesia). Coral reefs. 20 (4), pp. 399–408.

Andréfouët, S., Ouillon, S., Brinkman, R., Falter, J., Douillet, P., Wolk, F., Smith, R., Garen, P., Martinez, E., Laurent, V., LO, C., Remoissenet, G., Scourzic, B., Gilbert, A., Deleersnijder, E., Steinberg, C., Choukroun, S., Buestel, D., 2006. Review of solutions for 3D hydrodynamic modeling applied to aquaculture in South Pacific atoll lagoons. Marine pollution bulletin. 52. 1138-55. 10.1016.

Andréfouët, S., Guillaume, M.M.M., Delval, A., Rasoamanendrika, F.M.A., Blanchot, J., Bruggemann J.H., 2013. Fifty years of changes in reef flat habitats of the Grand Récif of Toliara (SW Madagascar) and the impact of gleaning. Coral Reefs, 32 (3), pp. 757-768. ISSN 0722-4028.

Angwenyi, C. M., Rydberg, L., 2005. Wave-driven circulation across the coral reef at bamburi lagoon, kenya. Estuarine, Coastal and Shelf Science. 63 (3), pp. 447–454.

Atkinson, M., Falter, J., Hearn, C., 2001. Nutrient dynamics in the Biosphere 2 coral reef mesocosm: water velocity controls NH4 and PO4 uptake. Coral Reefs 20, pp. 341-346.

Atkinson, M., Coleman, W. D., 1992. Policy Networks, Policy Communities and the Problems of Governance, Governance, 5, 2, 154-180.

Atkinson, M., Smith, S., Stroup, E., 1981. Circulation in enewetak atoll lagoon, Limnology and Oceanography 26 (6), pp. 1074–1083.

Aucan, J., Vendé-Leclerc, M., Dumas, P., Bricquir, M., 2017. Wave forcing and morphological changes of New Caledonia lagoon islets: Insights on their possible relations, Comptes Rendus Geoscience, Volume 349, Issues 6–7, 248-259, ISSN 1631-0713, https://doi.org/10.1016/j.crte.2017.09.003.

Battistini, R., Bourrouilh, F, Chevalier ,J.P., Coudray, J., Denizot, M., Faure, G., Fisher, G., Fisher, J.C., Guilcher, A., Harmelin-Vivien, M., Jaubert, J., Laborel, J., Montaggioni, L., Masse, J.P., Maugé, L. A., Peyrot-Clausade, M., Pichon, M., Plante, R., Plaziat, J.C., Plessis, Y. B., Richard G., Salvat, B., Thomassin, B. A., Vasseur, P., Weydert, P., 1975. Éléments de terminologie récifale indopacifique. Thetys, Vol. 7, n° 1, p. 1-111.

Blumberg, A. F., Mellor, G. L., 1987. A description of a three-dimensional coastal ocean circulation model, Three-Dimensional Coastal Ocean Models, vol. 208, N. Heap, New York, NY.

Bonneton, P., Lefebvre, J.P., Bretel, P., Ouillon, S., Douillet, P., 2007. Tidal modulation of wave-setup and wave-induced currents on the aboré coral reef, new caledonia. Journal of Coastal Research, 50, pp. 762–766.

Carassou, L., Le Borgne, R., Rolland, E., Ponton, D., 2010. Spatial and temporal distribution of zooplankton related to the environmental conditions in the coral reef lagoon of new caledonia, southwest pacific, Marine pollution bulletin 61 (7), pp. 367–374.

Chapman, A. C., 1985. Numerical treatment of cross-shelf open boundaries in a barotropic coastal ocean model, Journal Physical Oceanography 15, pp. 713–748.

Chevalier, C., Devenon, J. L., Pagano, M., Rougier, G., Blanchot, J., Arfi, R., 2017. The atypical hydrodynamics of the Mayotte Lagoon (Indian Ocean): effects on water age and potential impact on plankton productivity. Estuarine Coastal and Shelf Science, 196, pp. 182-197. ISSN 0272-7714.

Chevalier, C., Devenon, J. L., Rougier, G., Blanchot, J., 2015a. Hydrodynamics of the Toliara Reef Lagoon (Madagascar) : example of a lagoon influenced by waves and tides. Journal of Coastal Research, 31 (6), p. 1403-1416. ISSN 0749-0208

Chevalier, C., Sous, D., Devenon, J. L., Pagano, M., Rougier, G., Blanchot, J., 2015b. Impact of cross-reef water fluxes on lagoon dynamics: a simple parameterization for coral lagoon circulation model, with application to the Ouano Lagoon, New Caledonia. Ocean Dynamics. 65 (11), pp. 1509-1534. ISSN, 1616-7341.

De Brye, B., de Brauwere, A., Gourgue, O., Delhez, E. J. M., Deleersnijder, E., 2013. Reprint of Water renewal time scales in the Scheldt Estuary. Journal of Marine Systems, 128, pp 3-16, ISSN 0924-7963, https://doi.org/10.1016/j.jmarsys.2012.03.002.

Deleersnijder, E., 1992. Modélisation hydrodynamique tridimensionnelle de la circulation générale estivale de la région du détroit debering (in French), PhD thesis, Université Catholique de Louvain, Belgium.

Deleersnijder, E., Delhez, E. J. M., 2006. The Constituent-oriented Age and Residence time Theory (CART) - A holistic approach to the understanding of the results of complex marine results. 28 pages, working document, http://hdl.handle.net/2078.1/196274

Delhez, E. J., Campin, J.-M., Hirst, A. C., Deleersnijder, E., 1999. Toward a general theory of the age in ocean modelling. Ocean Modelling 1 (1), 17–27.

Delhez, E. J. M., de Brye, B., de Brauwere, A., Deleersnijder, E., 2014. Residence time vs influence time. Journal of Marine Systems, 132, pp. 185-195.

Delhez, E. J. M., Deleersnijder, E., 2002. The concept of age in marine modelling: II. Concentration distribution function in the English Channel and the North Sea. Journal of Marine Systems, 31, pp. 279-297.

Fernando, H., McCulley J., Mendis S., Perera K., 2005. Coral poaching worsens tsunami destruction in srilanka, Eos, Transactions American Geophysical Union. 86 (33), pp. 301–304.

Gourgue, O., Deleersnijder, E., White, F., 2007. Toward a generic method for studying water renewal, with application to the epilimnion of Lake Tanganyika. Estuarine Coastal and Shelf Science, 74, pp. 628-640

Gourlay, M.,1996a. Wave set-up on coral reefs. 1. set-up and wave-generated flow on an idealised two dimensional horizontal reef. Coastal Engineering 27 (3), pp. 161–193.

Gourlay, M., 1996b. Wave set-up on coral reefs. 2. set-up on reefs with various profiles, Coastal Engineering 28 (1), pp. 17–55.

Gourlay, M. R., Colleter, G., 2005. Wave-generated flow on coral reefs an analysis for two dimensional horizontal reef-tops with steep faces. Coastal Engineering 52 (4), pp. 353–387.

Haidvogel, D. B., Arango, H., Budgell, W. P., Cornuelle,B. D., Curchitser, E., Di Lorenzo,E., Fennel, K., Geyer, W. R., Hermann, A. J., Lanerolle, L., Levin, J., McWilliams, J.C., Miller, A. J., Moore, A. M., Powell, T. M., Shchepetkin, A. F., Sherwood,C. R., Signell, R. P., Warner, J. C., Wilkin J., 2008. Ocean forecasting in terrain-following coordonates: Formulation and skill assessment of the Regional Ocean Modeling System. Journal of Computational Physics, 227, pp. 3595-3624.

Hardy, T. A., Young, I. R., 1996. Field study of wave attenuation on an offshore coral reef. Journal of Geophysical Research: Oceans 101 (C6), pp. 14311–14326.

Hearn, C. J., 1999. Wave-breaking hydrodynamics within coral reef systems and the effect of changing relative sea level. Journal of Geophysical Research 104, pp. 30007-30020.

Hearn, C. J., Parker, I., 1988. Hydrodynamic processes on the ningaloo coral reef, western australia, in: Proceedings of the Sixth International Coral Reef Symposium, Vol. 2, pp. 497–502.

Hench, J. L., Leichter, J. J., Monismith, S. G., 2008. Episodic circulation and exchange in a wave-driven coral reef and lagoon system. Limnology and Oceanography. 53 (6), 2681.

Hoegh-Guldberg, Mumby, O., Hooten, P., Steneck, A.J., Greenfield, R.S., Gomez, P., Harvell, E., Sale, C., Edwards, P., Caldeira, A., Knowlton, K., Eakin, N., Prieto, C.M.I., Muthiga, R., Bradbury, N., Dubi, R., Hatziolos, A.M., 2008. Coral Reefs Under Rapid Climate Change and Ocean Acidification. Science (New York, N.Y.). 318. 1737-42. 10.1126/science.1152509.

Hoeke, R. K., Storlazzi, C. D., Ridd, P. V., 2013. Drivers of circulation in a fringing coral reef embayment: a wave-flow coupled numerical modeling study of Hanalei bay, Hawaii. Continental Shelf Research 58, pp. 79–95.

Hughes, T.P., Baird, A.H., Bellwood, D.R., 2003. Climate change, impacts, and the resilience of coral reefs. Science. 301, pp. 929-933.

Kärnä T., Baptista, A. M., 2016. Water age in the Columbia River estuary. Estuarine Coastal and Shelf Science 183, pp. 249–259

Kench, P., McLean, R., 2004. Hydrodynamics and sediment flux of hoa in an indian ocean atoll. Earth Surface Processes and Landforms. 29 (8), 933–953.

Kraines, S. B., Suzuki, A., Yanagi, T., Isobe, M., Guo, X., Komiyama, H., 1999. Rapid water exchange between the lagoon and the open ocean at majuro atoll due to wind, waves, and tide. Journal of Geophysical Research: Oceans 104 (C7), pp. 15635–15653.

Large, W. G., McWilliams,J. C., Doney, S. C., 1994. Oceanic vertical mixing: A review and a model with a nonlocal boundary layer parameterization. Reviews of Geophysics 32, pp. 363 – 403.

Liu, Y., MacCready, P, Hickey, B. M., Dever, E. P., Kosro, P. M., Banas, N. S., 2009. Evaluation of a coastal ocean circulation model for the Columbia River plume in summer 2004. Journal of Geophysical Research 114, C00B04, doi:10.1029/2008JC004929.

Longuet-Higgins, M.S.; Stewart, R.W., 1964. Radiation stresses in water waves; a physical discussion, with applications. Deep-Sea Research, 11 (4), pp. 529–562,

Lowe, R. J., Falter, J. L., Monismith, S. G., Atkinson, M. J., 2009. Wave-driven circulation of a coastal reef-lagoon system. Journal of Physical Oceanography 39 (4), pp. 873–893.

Lucas, L.V., Thompson, J.K., Brown, L.R., 2009. Why are diverse relationships observed between phytoplankton biomass and transport time? Limnology and Oceanography 54(1) , pp. 381-390.

Marchesiello, P., McWilliams, P., J., Shchepetkin, A., 2001: Open boundary conditions for long-term integration of regional oceanic models. Ocean Modelling,3, pp. 1–20.

Massel, S., Gourlay, M., 2000. On the modelling of wave breaking and set-up on coral reefs, Coastal Engineering 39 (1), pp. 1–27.

Masselink, G., 1998. Field investigation of wave propagation over a bar and the consequent generation of secondary waves. Coastal Engineering 33 (1). pp. 1–9.

Monismith, S. G., 2007. Hydrodynamics of coral reefs. Annual Review of Fluid Mechanics 39, pp. 37–55, https://doi.org/10.1146/annurev.fluid.38.050304.092125

Monismith, G., Herdman, L. M., Ahmerkamp, S., Hench, J. L., 2013. Wave transformation and wave-driven flow across a steep coral reef, Journal of Physical Oceanography, vol.43, issue.7, pp. 1356-1379.

Monismith, S. G., Rogers, J. S., Koweek, D., Dunbar, R. B., 2015. Frictional wave dissipation on a remarkably rough reef, Geophysical Research Letters, 42, 4063–4071, doi:10.1002/2015GL063804.

Ouillon, S., Douillet, P., Lefebvre, J.-P., Le Gendre, R., Jouon, A., Bonneton, P., Fernandez, J.-M., Chevillon, C., Magand, O., Lefe`vre, J., Le Hir, P., Laganier, R., Dumas, F., Marchesiello, P., Bel Madani, A., Andrefouet, S., Panche, J.-Y., Fichez, R., 2010. Circulation and suspended sediment transport in a coral reef lagoon: the southwest lagoon of New Caledonia. Marine Pollution Bulletin 61, 269–296, http://dx.doi.org/10.1016/j.marpolbul.2010.06.023.

Pagano, M., Rodier, M., Guillaumot, C., Thomas, Y., Henry, K., Andrefouet, S., 2017. Ocean-lagoon water and plankton exchanges in a semi-closed pearl farming atoll lagoon (Ahe, Tuamotu archipelago, French Polynesia). Estuarine Coastal and Shelf Science, 191, pp. 60-73.

Pandolfi, J.B., Sala,R., Hughes, E., Bjorndal, T., Cooke, K., McArdle, R., Mcclenachan, D., Newman, L., Paredes, M., Warner, G., Jackon, R.J., 2003. Global Trajectories of the Long -Term Decline of Coral Reef Ecosystems. Science (New York, N.Y.). 301. 955-8. 10.1126/science.1085706.

Penven, P., Debreu, L., Marchesiello, P., McWilliams, J.C., 2006. Evaluation and Application of the TOMS 1-way embedding procedure to the central California upwelling system. Ocean Modelling, 12, pp. 157-187.

Pomeroy, A., Lowe, R., Symonds, G., Van Dongeren, A., Moore, C., 2012. The dynamics of infragravity wave transformation over a fringing reef. Journal of Geophysical Research: Oceans 117 (C11).

Roberts, H.H., Suhayda J.N., 1983. Wave-current interactions on a shallow reef (Nicaragua, Central America). Coral Reefs 1(4), pp. 209–214.

Sous D., Chevalier Cristèle, Devenon J. L., Blanchot J., Pagano M., 2017. Circulation patterns in a channel reef-lagoon system, Ouano lagoon. New Caledonia. Estuarine Coastal and Shelf Science, 196, pp. 315-330. ISSN 0272-7714

Symonds, G., Black, K. P., Young, I. R., 1995. Wave-driven flow over shallow reefs. Journal of Geophysical Research: Oceans 100 (C2), pp. 2639–2648.

Szmant, A. M., 2002. Nutrient enrichment on coral reefs: is it a major cause of coral reef decline? Estuaries 25 (4), pp. 743–766.

Taebi, S., Lowe, R. J., Pattiaratchi, C. B., Ivey, G. N., Symonds, G., Brinkman, R., 2011. Nearshore circulation in a tropical fringing reef system. Journal of Geophysical Research: Oceans (1978–2012) 116 (C2).

Tartinville, B., Rancher, J., 2000. Wave-induced flow over mururoa atoll reef. Journal of Coastal Research, pp. 776–781.

Tolman, H. L., 2006: Development of a multi-grid version of WAVEWATCH III. NOAA / NWS / NCEP / MMAB Technical Note 256, 88 pp.+ Appendices.

Willmott, C.J., 1981.On the validation of models. Physical Geography 2 (2), pp. 184–194

Wolanski, E., Delesalle, B., Dufour, V., Aubanel, A., 1993. Modeling the fate of pollutants in the tiahura lagoon, moorea, french polynesia, in: 11th Australasian Conference on Coastal and Ocean Engineering: Coastal Engineering a Partnership with Nature ; Preprints of Papers, Institution of Engineers, Australia, 1993, pp. 583-588.

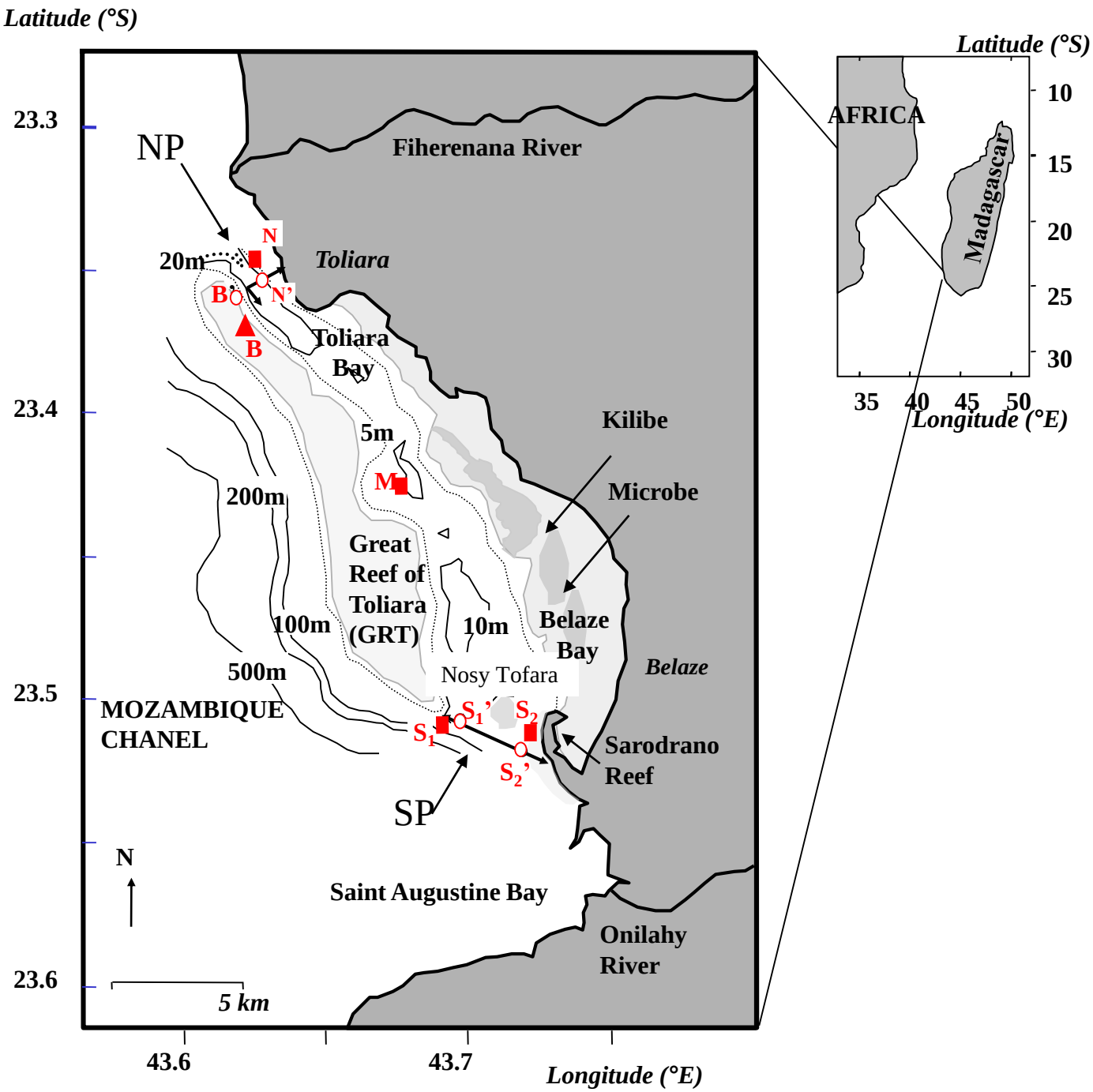
Latitude (°S)
23.3
23.4
23.5
23.6
NP
Fiherenana River
N
20m
Toliara
B'
N'
B
Toliara
Bay
5m
M
200m
Kilibe
Microbe
Great
Reef of
Toliara
(GRT)
100m
10m
Belaze
Bay
Belaze
500m
Nosy Tofara
MOZAMBIQUE
CHANEL
S1'
S2
S1
S2'
Sarodrano
Reef
SP
N
Saint Augustine Bay
Onilahy
River
5 km
43.6
43.7
Longitude (°E)
Latitude (°S)
AFRICA
Madagascar
10
15
20
25
30
35
40
45
50
Longitude (°E)

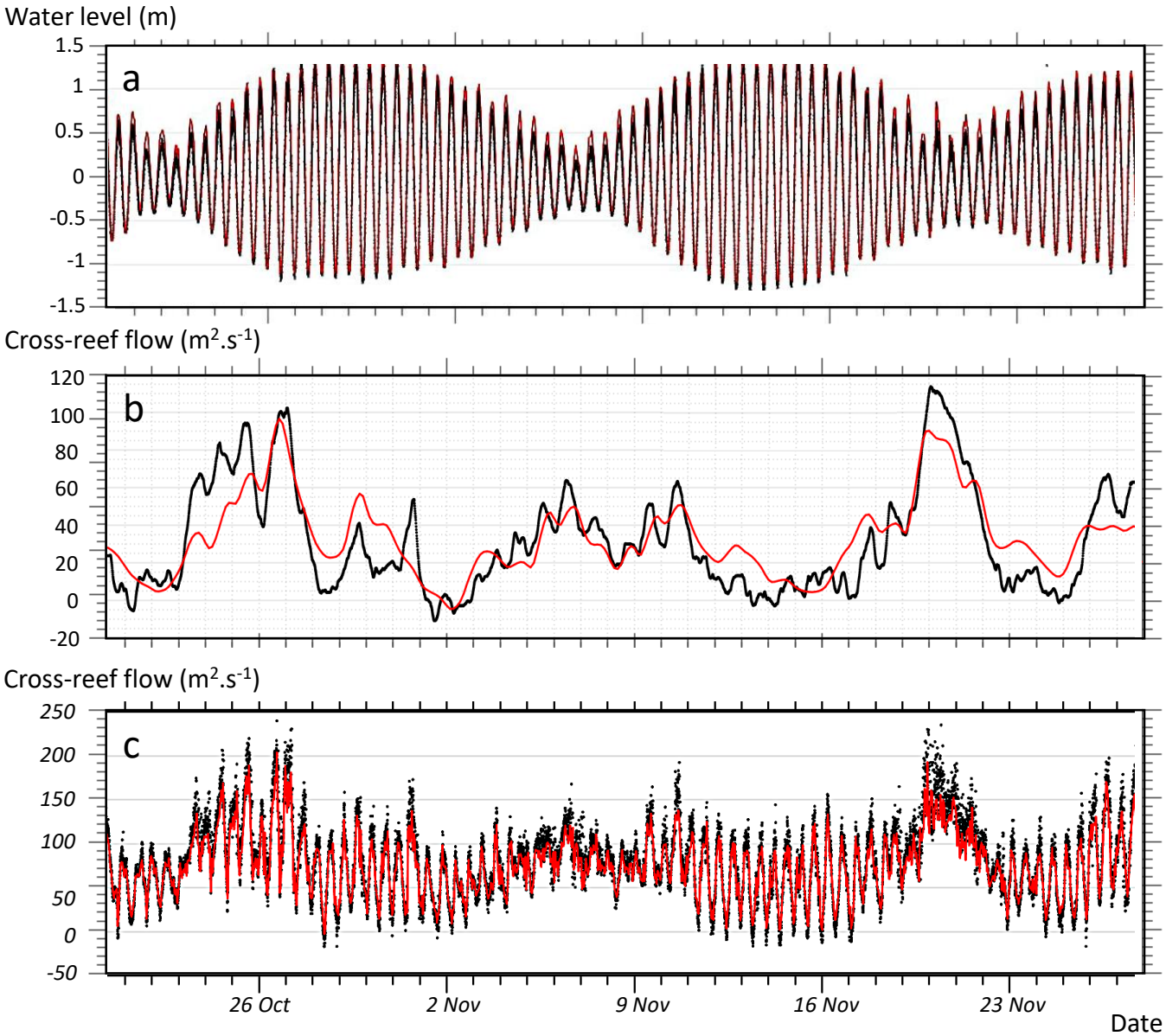
Water level (m)
a
1.5
1
0.5
0
-0.5
-1
-1.5
Cross-reef flow (m².s⁻¹)
b
120
100
80
60
40
20
0
-20
Cross-reef flow (m².s⁻¹)
c
250
200
150
100
50
0
-50
26 Oct
2 Nov
9 Nov
16 Nov
23 Nov
Date

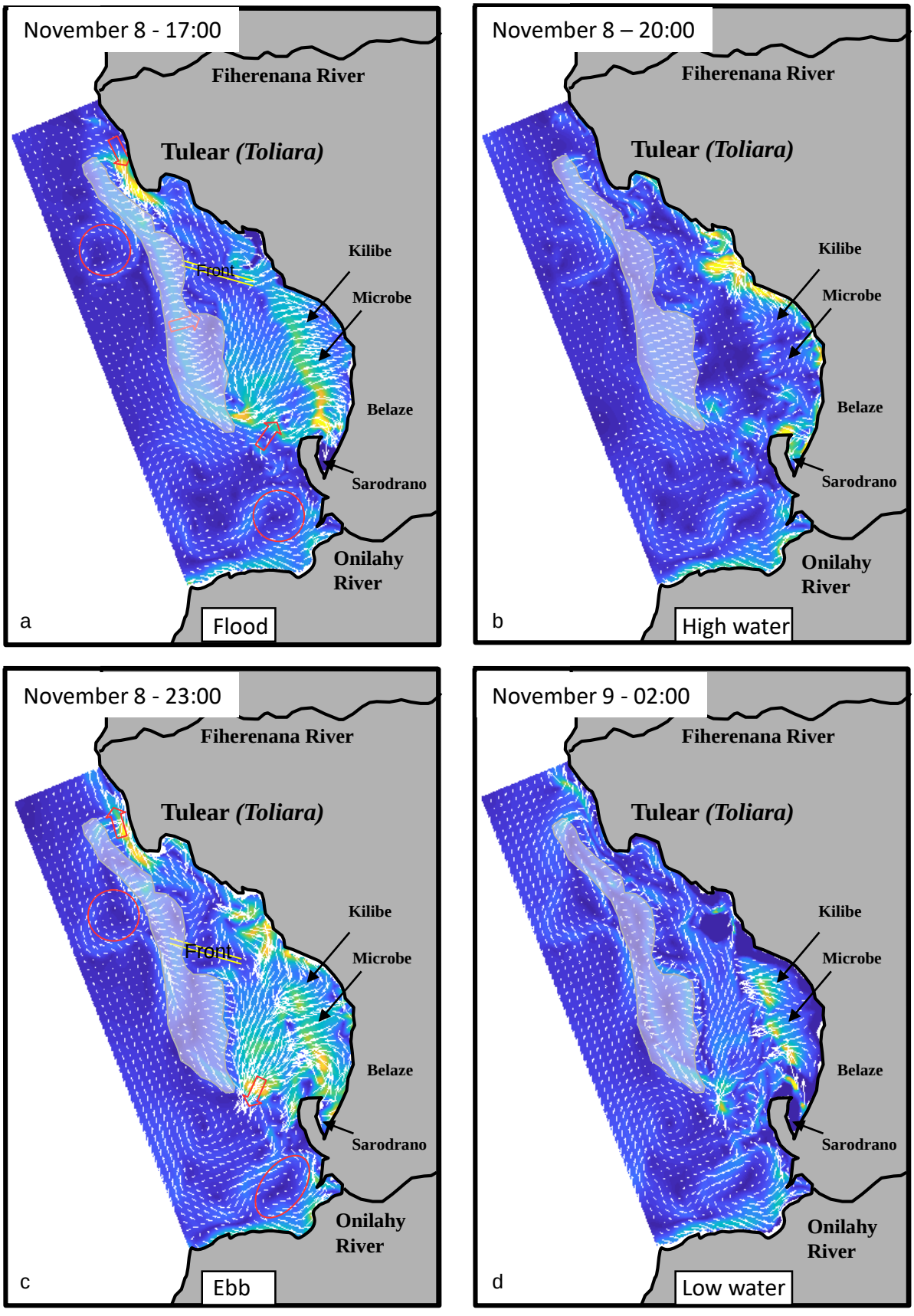
November 8 - 17:00
Fiherenana River
Tulear (Toliara)
Front
Kilibe
Microbe
Belaze
Sarodrano
Onilahy River
a
Flood
November 8 – 20:00
Fiherenana River
Tulear (Toliara)
Kilibe
Microbe
Belaze
Sarodrano
Onilahy River
b
High water
November 8 - 23:00
Fiherenana River
Tulear (Toliara)
Front
Kilibe
Microbe
Belaze
Sarodrano
Onilahy River
c
Ebb
November 9 - 02:00
Fiherenana River
Tulear (Toliara)
Kilibe
Microbe
Belaze
Sarodrano
Onilahy River
d
Low water
Velocity (m.s-1)
0
0.1
0.2
0.3
0.4
0.5

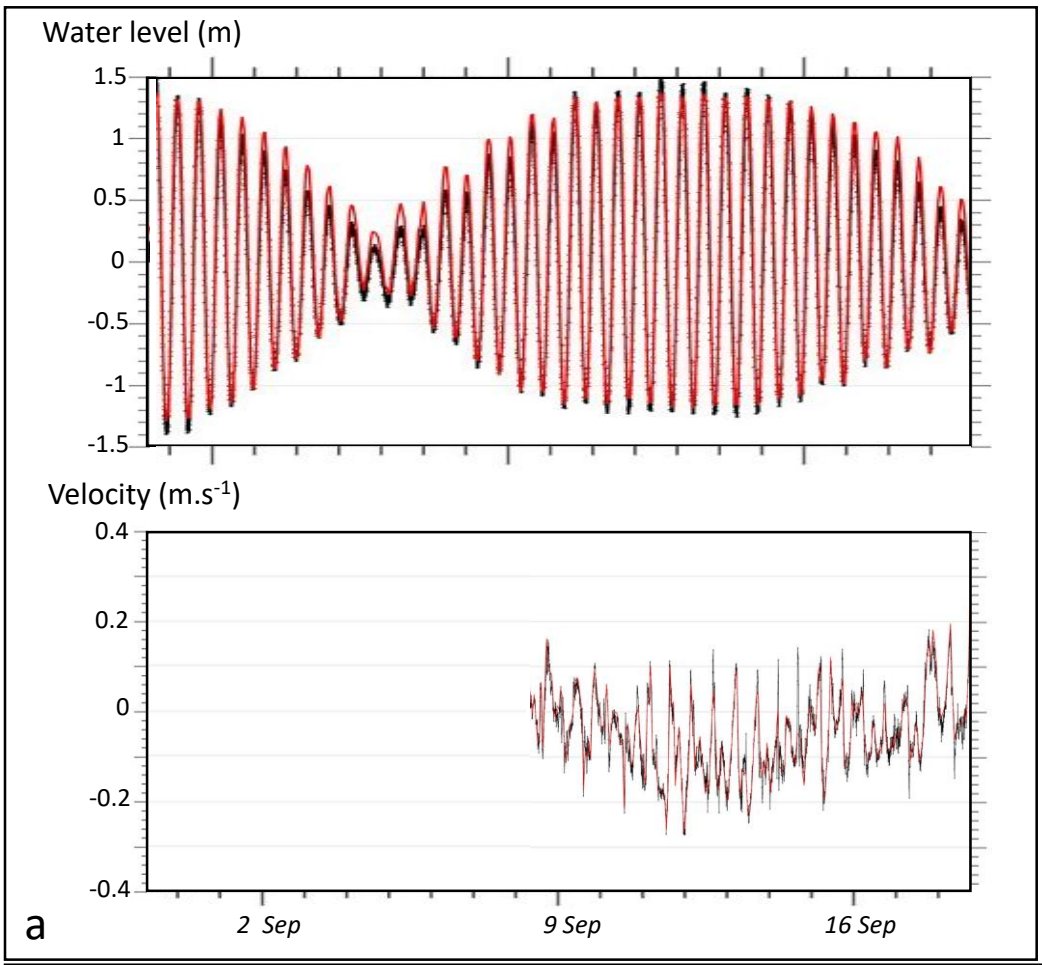
Water level (m)
1.5
1
0.5
0
-0.5
-1
-1.5
Velocity (m.s-1)
0.4
0.2
0
-0.2
-0.4
2 Sep
9 Sep
16 Sep
a

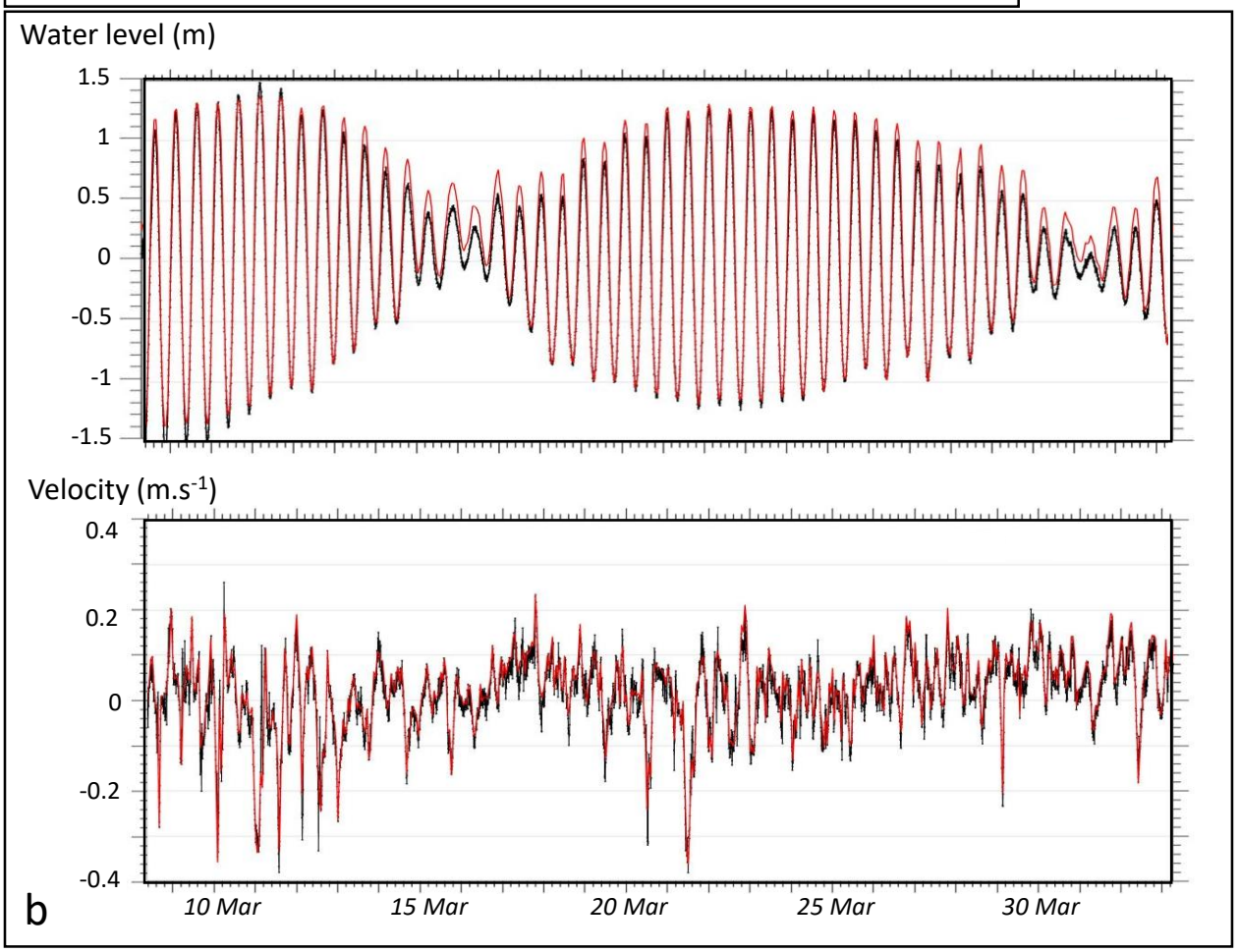
Water level (m)
1.5
1
0.5
0
-0.5
-1
-1.5
Velocity (m.s-1)
0.4
0.2
0
-0.2
-0.4
10 Mar
15 Mar
20 Mar
25 Mar
30 Mar
b

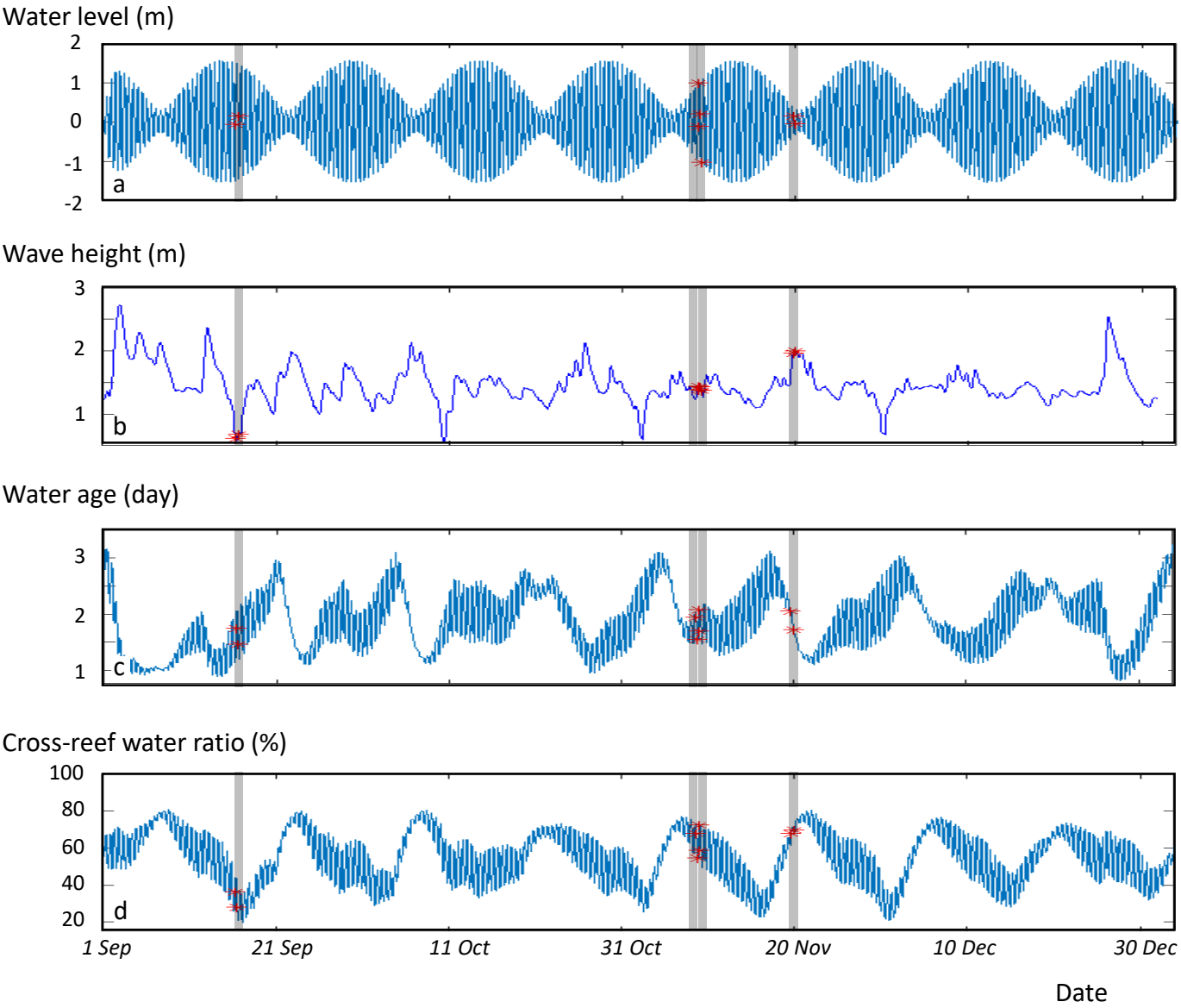
Water level (m)
2
1
0
-1
-2
a
Wave height (m)
3
2
1
b
Water age (day)
3
2
1
c
Cross-reef water ratio (%)
100
80
60
40
20
d
1 Sep
21 Sep
11 Oct
31 Oct
20 Nov
10 Dec
30 Dec
Date

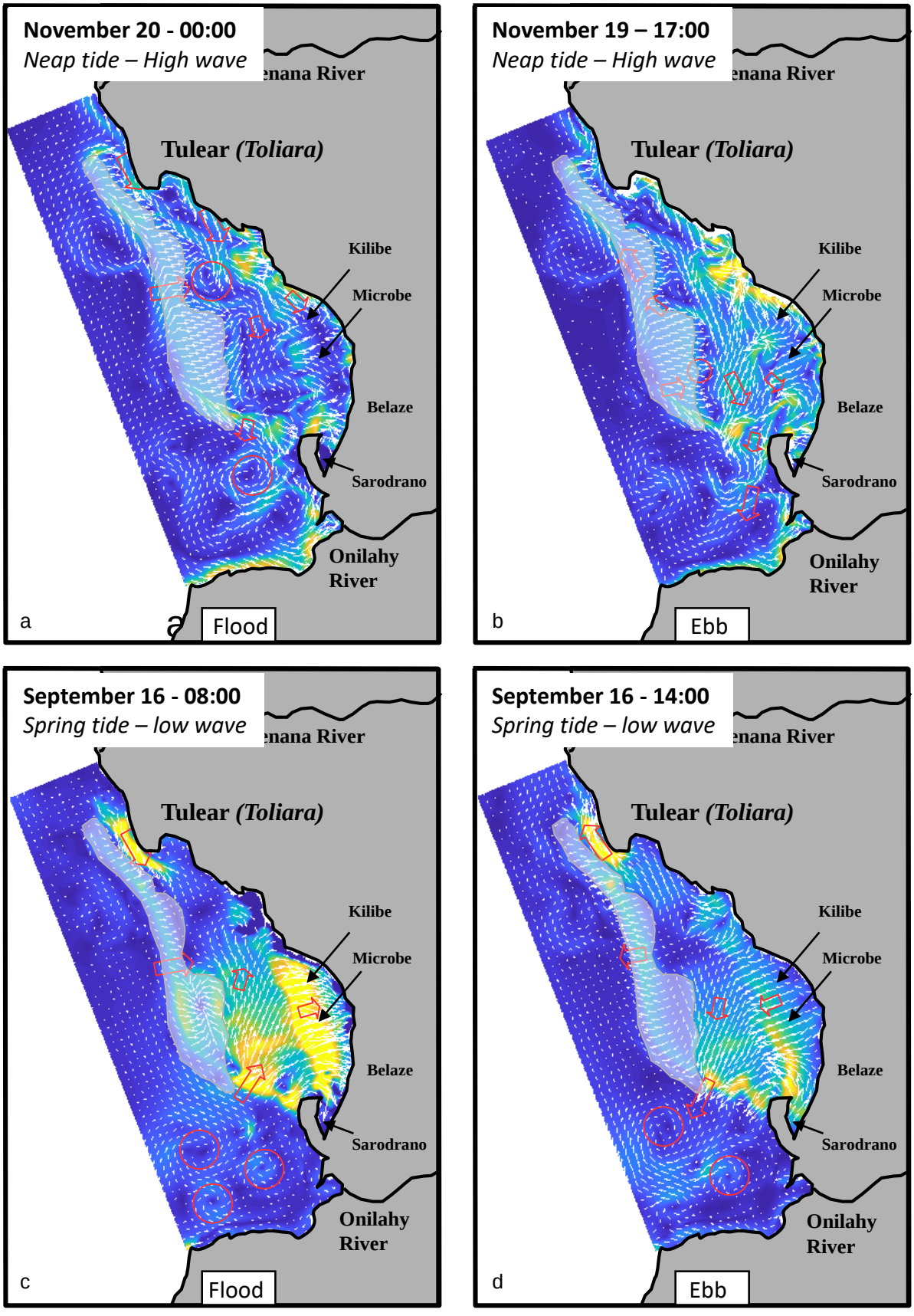
November 20 - 00:00
Neap tide – High wave
Tulear (Toliara)
Kilibe
Microbe
Belaze
Sarodrano
Onilahy River
a
Flood
November 19 – 17:00
Neap tide – High wave
Tulear (Toliara)
Kilibe
Microbe
Belaze
Sarodrano
Onilahy River
b
Ebb
September 16 - 08:00
Spring tide – low wave
Tulear (Toliara)
Kilibe
Microbe
Belaze
Sarodrano
Onilahy River
c
Flood
September 16 - 14:00
Spring tide – low wave
Tulear (Toliara)
Kilibe
Microbe
Belaze
Sarodrano
Onilahy River
d
Ebb
Velocity (m.s-1)
0
0.1
0.2
0.3
0.4
0.5

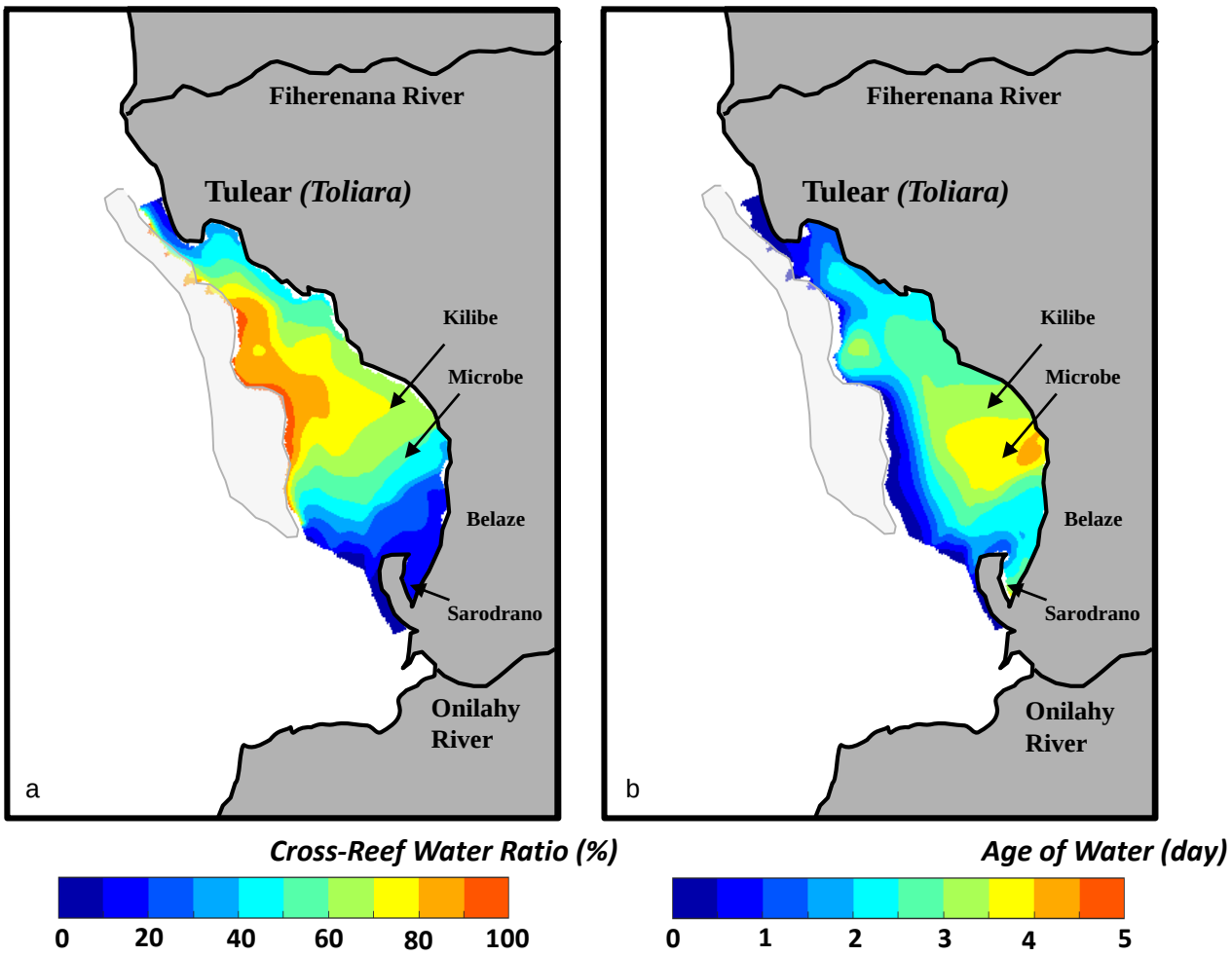
Fiherenana River
Tulear (Toliara)
Kilibe
Microbe
Belaze
Sarodrano
Onilahy River
a
Fiherenana River
Tulear (Toliara)
Kilibe
Microbe
Belaze
Sarodrano
Onilahy River
b
Cross-Reef Water Ratio (%)
0
20
40
60
80
100
Age of Water (day)
0
1
2
3
4
5

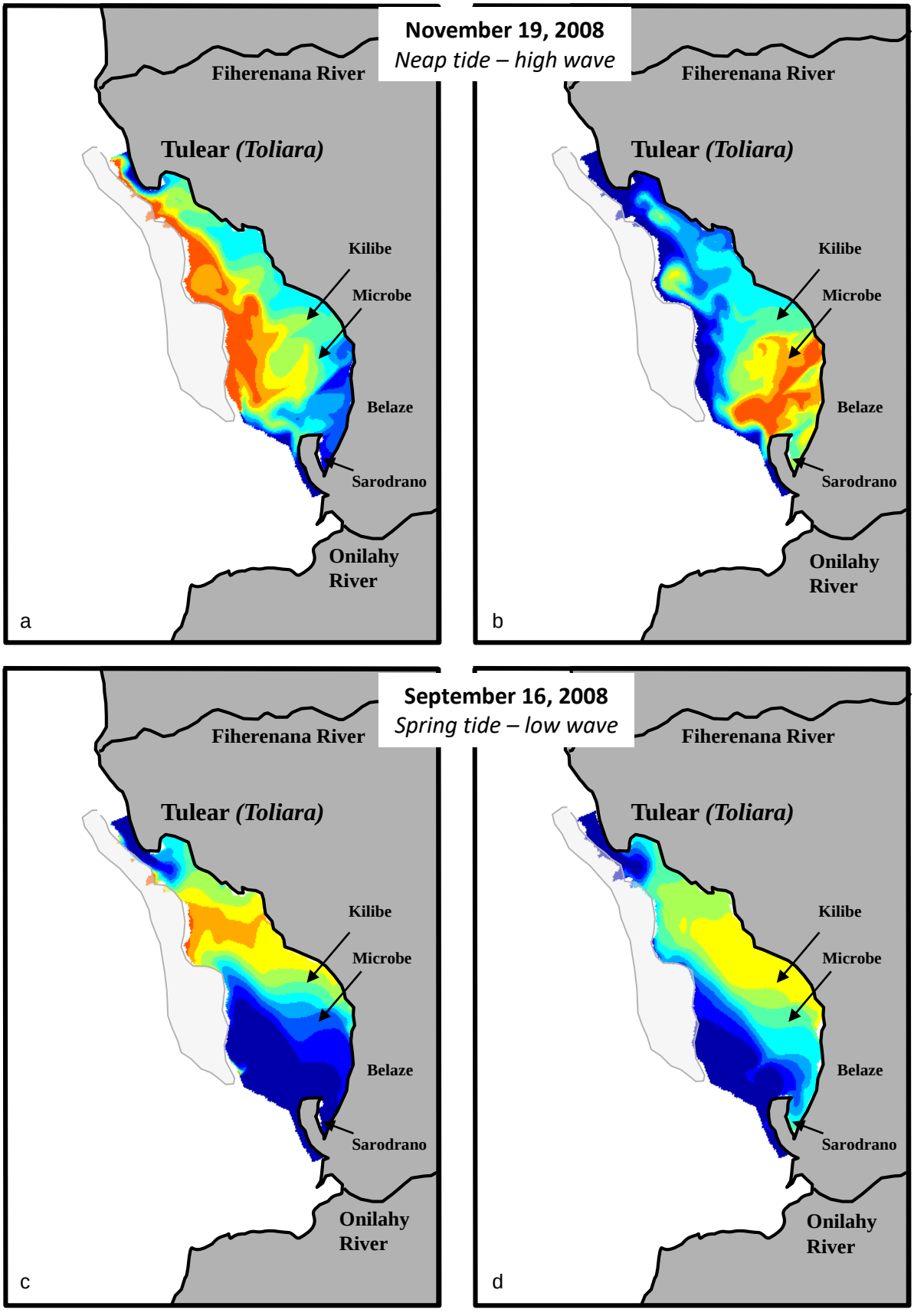
November 19, 2008
Neap tide – high wave
Fiherenana River
Tulear (Toliara)
Kilibe
Microbe
Belaze
Sarodrano
Onilahy River
a
b
September 16, 2008
Spring tide – low wave
c
d
Cross-Reef Water Ratio (%)
0
20
40
60
80
100
Age of Water (day)
0
1
2
3
4
5

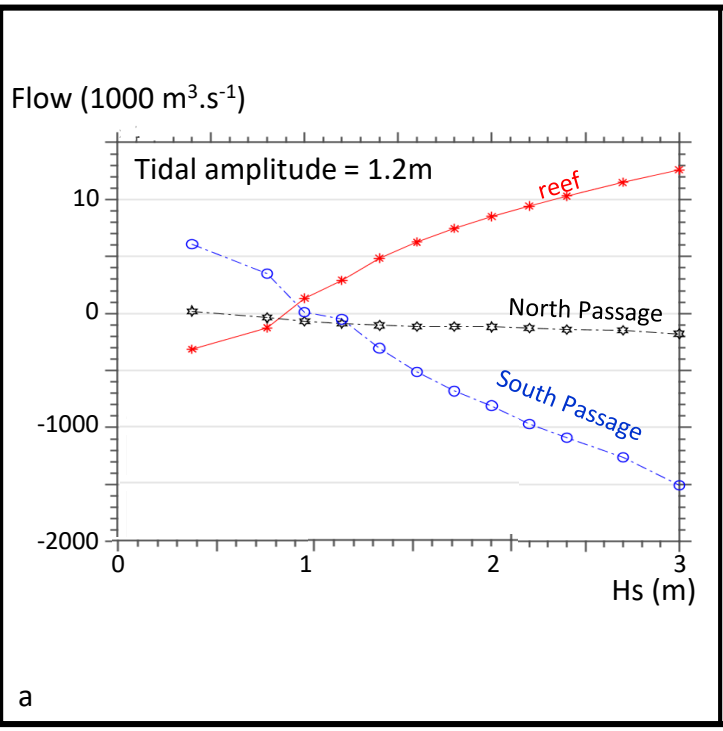
Flow (1000 m3.s-1)
Tidal amplitude = 1.2m
reef
North Passage
South Passage
10
0
-1000
-2000
0
1
2
3
Hs (m)

a

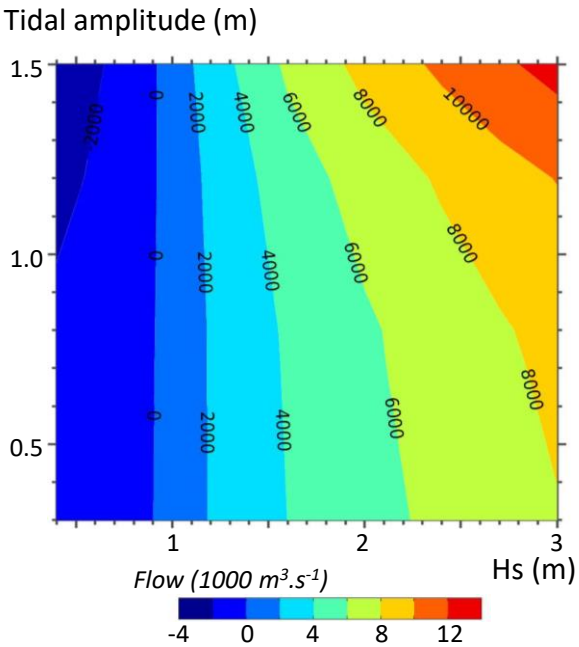
Tidal amplitude (m)
1.5
1.0
0.5
-2000
0
2000
4000
6000
8000
10000
1
2
3
Hs (m)
Flow (1000 m3.s-1)
-4
0
4
8
12

b

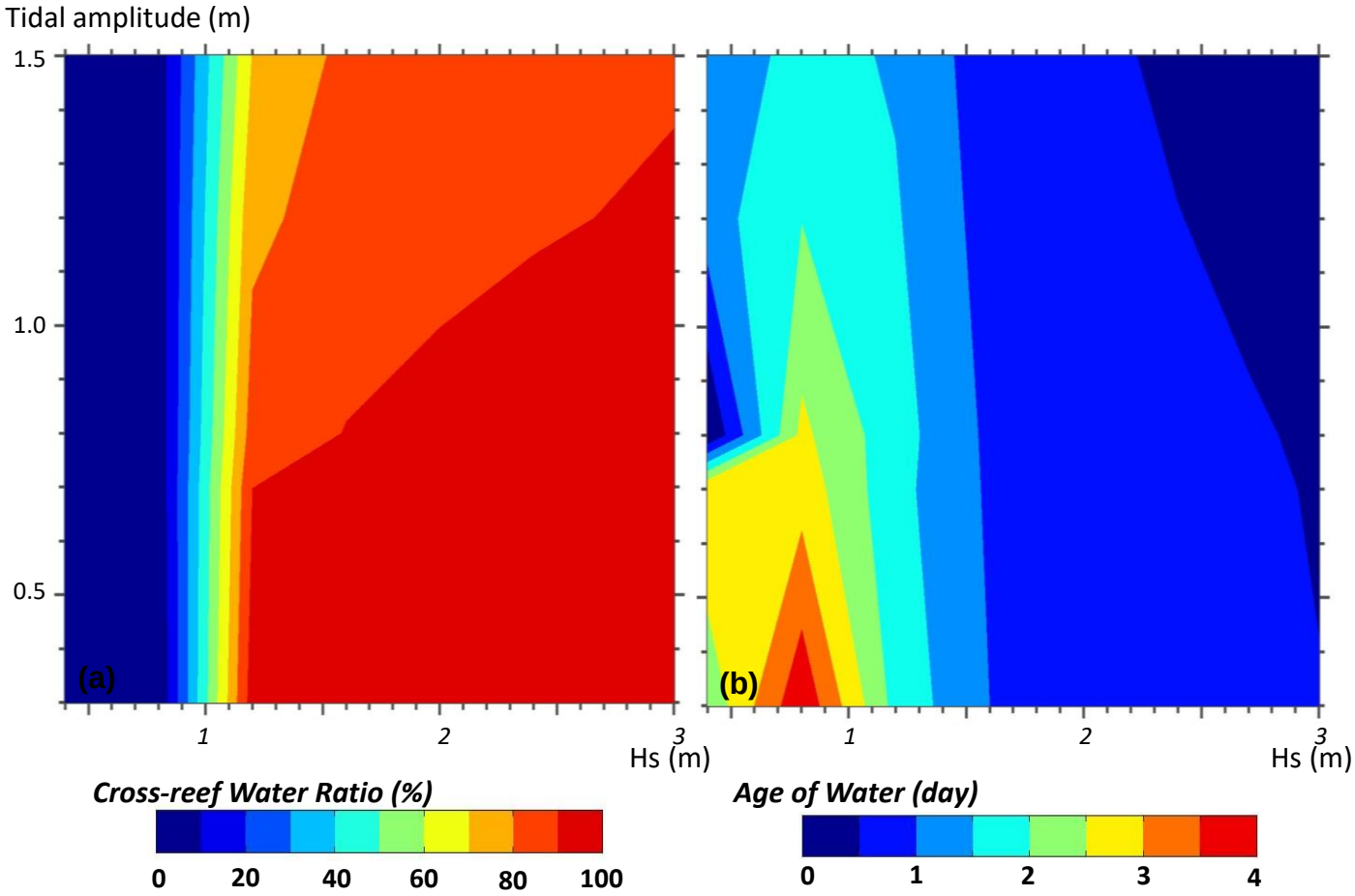
Tidal amplitude (m)
1.5
1.0
0.5
(a)
(b)
1
2
3
Hs (m)
Cross-reef Water Ratio (%)
0
20
40
60
80
100
Age of Water (day)
0
1
2
3
4

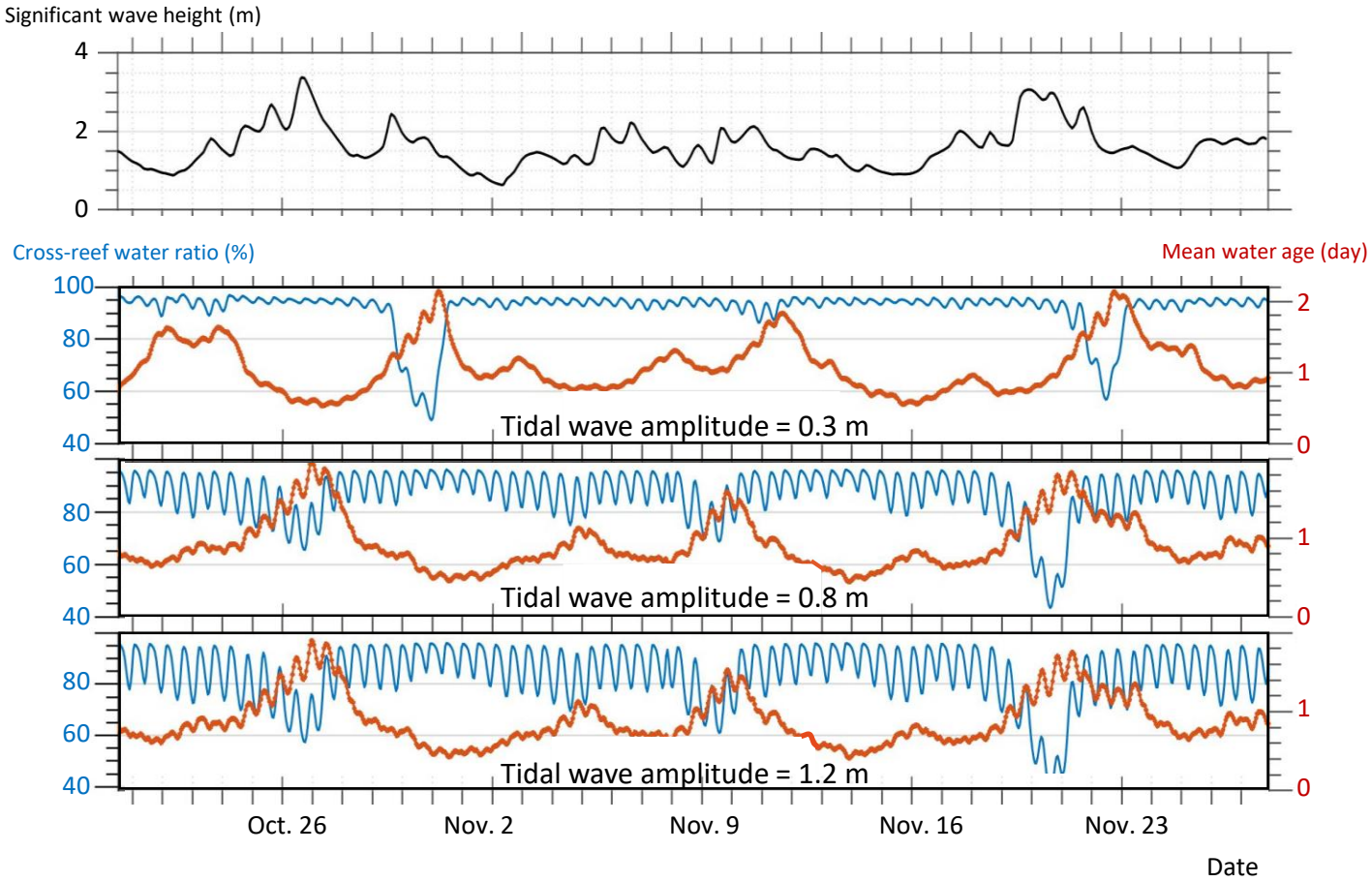
Significant wave height (m)
4
2
0
Cross-reef water ratio (%)
Mean water age (day)
100
80
60
40
2
1
0
Tidal wave amplitude = 0.3 m
Tidal wave amplitude = 0.8 m
Tidal wave amplitude = 1.2 m
Oct. 26
Nov. 2
Nov. 9
Nov. 16
Nov. 23
Date

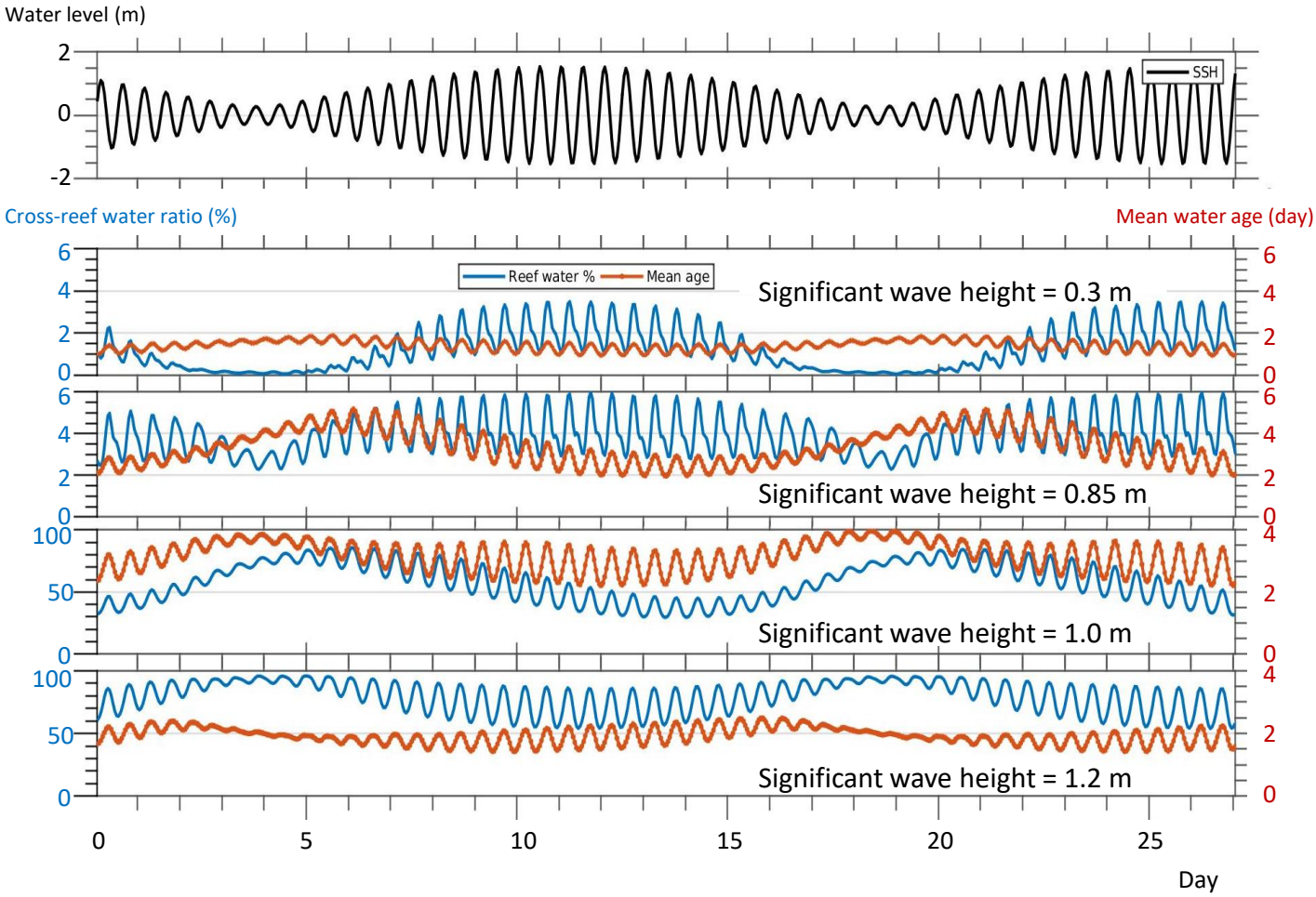
Water level (m)
SSH
Cross-reef water ratio (%)
Mean water age (day)
Reef water %
Mean age
Significant wave height = 0.3 m
Significant wave height = 0.85 m
Significant wave height = 1.0 m
Significant wave height = 1.2 m
Day

Table 1: Discrepancy of tidal amplitude and tidal phase between simulated results and observations of water level and velocity in the main direction

			Amplitude			Phase		
			Data	Model	Error (%)	Data	Model	Error
Campaign 1								
N	Water level	M2	0.81	0.78	3.70	57.00	57.69	0.68
		S2	0.62	0.63	1.61	95.00	96.32	1.32
	Velocity	M2	0.34	0.33	2.94	185.67	184	1.67
		S2	0.30	0.28	6.67	204.77	203	1.77
S2	Water level	M2	0.78	0.74	5.12	62.00	60.74	1.26
		S2	0.60	0.62	3.33	96.00	97.01	0.93
	Velocity	M2	0.27	0.29	7.41	325.79	324	1.79
		S2	0.21	0.23	9.52	357.23	359	1.76
S1	Water level	M2	0.69	0.74	7.26	66.00	61.00	5.20
		S2	0.66	0.62	6.06	95.76	100.83	5.07
	Velocity	M2	0.29	0.32	10.34	302.68	306	3.33
		S2	0.19	0.21	10.53	341.16	347	5.85
M	Water level	M2						
		S2						
	Velocity	M2	0.07	0.06	14.30	233.48	240	6.52
		S2	0.10	0.09	10.00	249.75	254	4.25
Campaign 2								
N’	Water level	M2	0.76	0.78	2.63	56.00	56.12	0.12
		S2	0.58	0.63	8.62	97.00	96.77	0.24
	Velocity	M2	0.35	0.39	11.43	187.08	186	1.08
		S2	0.29	0.26	10.35	243.73	242	1.74
S1’	Water level	M2	0.83	0.74	10.48	61.00	61.12	0.12
		S2	0.61	0.63	3.28	100.00	100.99	0.99
	Velocity	M2	0.44	0.39	11.36	323.18	322	1.18
		S2	0.40	0.33	17.50	358.96	357	1.96
S2’	Water level	M2	0.82	0.74	9.76	61.00	60.88	0.12
		S2	0.64	0.62	3.12	102.00	100.73	1.27
	Velocity	M2	0.12	0.14	16.67	293.25	289	4.25
		S2	0.15	0.13	13.33	330.75.	328	2.75
Campaign 3								
B	Water level	M2	0.80	0.78	2.50	58.00	57.78	0.22
		S2	0.59	0.63	6.78	96.00	96.59	0.59
	Velocity	M2	0.11	0.09	9.09	146.40	148	1.60
		S2	0.06	0.05	16.68	139.78	141	1.22

Table 2: Descriptive statistics of the model accuracy in reproducing observed cross-shore and along-shore velocities by mean of the RMSE (m) and skill values at tidal gauge stations.

Campaign	Gauge station	Skill			RMSE		
		U	V	Water Level	U	V	Water Level
C1	N	0.95	1	0.97	0.06	0.01	0.02
	S2	0.94	0.98	1	0.03	0.02	0.02
	S1	0.99	1	0.99	0.05	0.02	0.05
	M	0.67	0.99		0.08	0.01	
C2	N’	0.96	1	0.98	0.05	0.02	0.02
	S1’	0.95	1	1	0.03	0.02	0.06
	S2’	0.93	0.98	0.99	0.02	0.03	0.02
C3	B	0.97	0.95	0.98	0.01	0.04	0.01

Table 3a: Set of simulations.

	Date	Significant wave height	Tidal amplitude	Duration Simulations (after spin-up)	Spin-up	Simulations Number
Sensitivity Simulations	/	Constant from 0 to 3 m	Constant from 0.3 m to 1.5 m	30 days	5 days	125
Semi-realistic Simulations	2008 : October 20 - November 27 - campaign C3	Constant : 0.3m; 0.85m; 1m; 1.2m	Realist tide (from 0.3m to 1.5m)	30 days	5 days	4
	2008 : October 20 - November 27 - campaign C3	Realist wave (from 0.64m to 1.5m)	Constant : 0.3m; 0.8m; 1.2m	39 days	5 days	3
Realist Simulations	2007 : August 23 -October 13 - campaign C1	Realist wave (from 0.64m to 1.5m) - campaign C1	Realist tide (from 0.3m to 1.5m)	52 days	5 days	1
	2008 : March 3 - April 4 - campaign C2	Realist wave (from 0.64m to 1.5m) - campaign C2	Realist tide (from 0.3m to 1.5m)	33 days	5 days	1
	2008 : October 20 - November 27 - campaign C3	Realist wave (from 0.64m to 1.5m) - campaign C3	Realist tide (from 0.3m to 1.5m)	39 days	5 days	1

Table 3b: Sensitivity simulations set

		Significant wave height																																																												
		0m				*0.2m*				*0.4m*				*0.6m*				*0.8m*				*1m*				*1.2m*				*1.4m*				*1.6m*				*1.8m*				*2m*				*2.2m*				*2.4m*				*2.6m*				*2.8m*				*3m*
Tidal amplitude	*0.3m*	■						■										■				■				■				■				■				■				■				■				■						■						■
	0.7m	■						■										■				■				■				■				■				■				■				■				■						■						■
	0.8m	■	■	■	■	■	■	■	■	■	■	■	■	■	■	■	■	■	■	■	■	■	■	■	■	■	■	■	■	■	■	■	■	■	■	■	■	■	■	■	■	■	■	■	■	■	■	■	■	■	■	■	■	■	■	■	■	■	■	■	■	■
	0.9m	■						■										■				■				■				■				■				■				■				■				■						■						■
	1.2m	■						■										■				■				■				■				■				■				■				■				■						■						■
	1.5m	■						■										■				■				■				■				■				■				■				■				■						■						■